Particle channeling in a bent crystal

A. M. Taratin
Joint Institute for Nuclear Research, Dubna

Fiz. Élem. Chastits At. Yadra **29**, 1063–1118 (September–October 1998)

The channeling of high-energy charged particles in bent crystals is being used more and more extensively for steering particle beams at accelerators, for extracting a beam or its halo from an accelerator, and for splitting the extracted beam. The use of the strong intracrystalline fields of bent crystals in high-energy physics, for example, to measure the magnetic moments of short-lived particles from the spin precession angle in a bent crystal, appears to be very promising. The results of studies on the channeling of high-energy particles in a bent crystal are reviewed. The features of channeling and quasichanneling, the ionization energy losses, and the radiation emitted by channeled particles are studied. The possibility of polarization effects for channeled particles is discussed. © *1998 American Institute of Physics.* [S1063-7796(98)00105-3]

1. INTRODUCTION

The channeling effect is manifested in the passage of fast charged particles through an oriented single crystal[1)] (Ref. 1). If we look at a crystal lattice along the direction of dense packing, we see a two-dimensional lattice formed by rows of atoms. A positively charged particle entering the crystal at a small angle relative to the direction of dense packing moves along the rows of atoms without closely approaching them, owing to repulsion in correlated small-angle collisions with the atoms of a row. Planar channeling occurs when the transverse momentum of the incident particle is directed along a densely packed plane of the crystal. In this case the particle moves while oscillating between adjacent crystal planes. For channeled particles, the yield of processes requiring near collisions with atoms is decreased, the ionization energy losses and particle multiple scattering are decreased, and the particle mean free paths are increased.

The motion of channeled particles is controlled by the average electric field of the crystal atoms along the crystallographic axes or planes. The idea of using intracrystalline fields for controlling beams of high-energy charged particles by means of bent single crystals is due to Tsyganov of the JINR (1976; Ref. 2). It was assumed that in planar channeling, positively charged particles would follow the bending of the crystal up to some critical bend radius determined by the maximum strength $\mathscr{E}_{\max}$ of the atomic electric field averaged along the planes:

$$R_c=\frac{E}{e\mathscr{E}_{\max}}, \tag{1}$$

where E is the particle energy. For example, for the (110) channel of a silicon crystal, $\mathscr{E}_{\max}\simeq 6$ GV/cm, and for 1-TeV protons, $R_c=1.6$ m.

In 1978 the deflection of channeled particles by a bent crystal was discovered in a computer experiment using the binary-collision model, which allows detailed reproduction of the particle trajectory in a crystal.[3] In addition to the planar channeling regime for positively charged particles, the deflection effect was also discovered in axial channeling for positively and negatively charged particles.

In 1979 the possibility of steering beams of charged particles using bent crystals was first demonstrated[4] in an experiment on the deflection of a beam of 8.4-GeV protons extracted from the synchrophasotron of the Laboratory of High Energies, JINR (see Fig. 1). At the same time, an experiment was performed[5] on the deflection of 900-MeV electrons at the Institute of Nuclear Physics, Tomsk Polytechnic Institute, and somewhat later at CERN[6] using a beam of secondary particles of momentum up to 12 GeV/c. In 1984 a bent crystal was used for the first time to extract a circulating proton beam from the synchrophasotron of the Laboratory of High Energies, JINR.[7] The deflection and extraction of a particle beam from a cyclic accelerator by a bent crystal was later studied at IHEP,[8,9] CERN,[10,11] and Fermilab.[12,13] A beam extraction efficiency of 20–30% was attained.

These studies showed that practical applications of crystals for steering particle beams are promising. For example, at the IHEP synchrotron the crystal extraction system functions continuously, which broadens the possibilities for performing experiments, and the setup for splitting the extracted proton beam using bent crystals is used to organize simultaneous studies in several experimental channels. The possibility of focusing a particle beam by a bent crystal and the use of such a crystal for beam parameter diagnostics have been demonstrated experimentally.[9] A bent crystal has been used to deflect a beam of relativistic carbon nuclei extracted from the JINR synchrophasotron to the experimental setup.[14]

The use of crystal deflectors at the proton and heavy-ion colliders UNK, LHC, and RHIC appears to be very promising. Here it is possible to extract particles from the beam halo for simultaneous fixed-target experiments without interfering with the collider regime. In this case the crystal can operate as a scraper. Such a crystalline scraper–deflector in a loss-localization system can drastically decrease the radiation background of collider experiments.[15]

In addition to crystal-optics systems, bent crystals can be

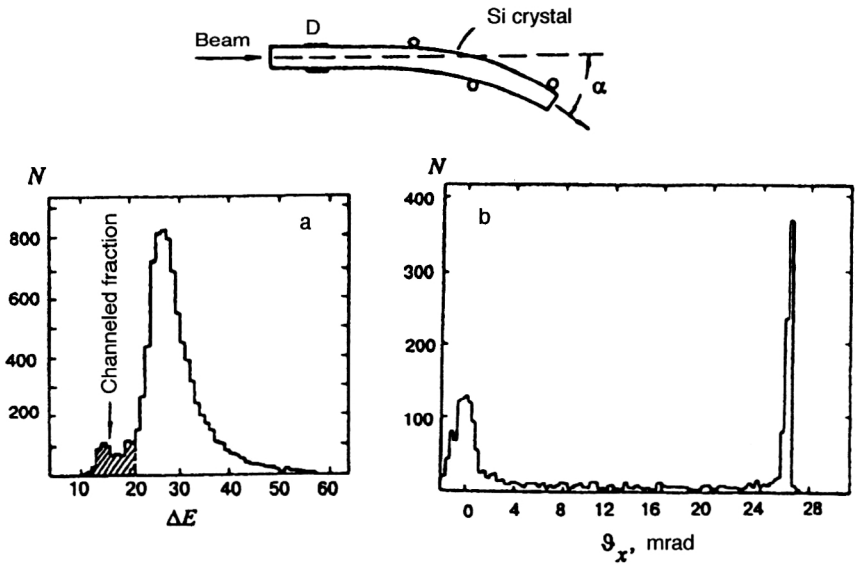

FIG. 1. Discovery of particle deflection by a bent crystal in an 8.4-GeV proton beam at the JINR synchrophasotron. The upper figure schematically shows the bent crystal: D is a surface-barrier detector allowing the selection of channeled particles according to the ionization losses. (a) Full spectrum of particle ionization losses; (b) distribution of proton deflection angles for the channeled fraction.

used in actual physical experiments to measure particle energies from the synchrotron radiation,[16] to measure the magnetic moments of short-lived particles from their spin precession,[17] and to create polarized high-energy electron and positron beams.[18]

In this review we study the main features of particle channeling in a bent crystal. We limit ourselves to planar channeling, owing to its importance for practical applications and because it has been fairly well studied. We discuss the effect of crystal bending on particle dechanneling, on processes involving quasichanneled particles, on the radiation and ionization energy losses of channeled particles, and on the possibility of polarization phenomena for channeled particles in the average electric field of the crystal planes. Detailed discussions of the experimental studies and practical applications of bent crystals for controlling beams of high-energy particles can be found in Refs. 9 and 19–21.

2. CLASSICAL CHANNELING THEORY

Within the framework of classical mechanics, Lindhard[1] developed a theory of the orientational effects of fast charged particles in crystals, which successfully explained the experimental results which had been obtained by that time.

The adequacy of the classical description of particle scattering on an individual atom, i.e., the condition of well-defined classical trajectory, when the transverse dimensions of the wave packet are much smaller than the dimensions of the scattering field, $\Delta b \ll r_a$, and the associated uncertainty in the scattering angle $\Delta\theta$ is small compared with the scattering angle, $\Delta\theta \ll \theta$, is violated already for a proton of energy ~ 1 MeV. In passing through matter, the width of the particle wave packet grows rapidly in a series of successive collisions with the atoms.

The situation is different in particle channeling in a crystal. A channeled particle moves at a small angle along the atomic rows or planes, undergoing correlated collisions with the atoms, so that the impact parameter in successive collisions changes only slightly. In such a series of correlated collisions with atoms the uncertainty in the scattering angle and the transverse coordinate does not grow additively with the contributions from individual collisions, and the width of the wave packet of a channeled particle remains nearly unchanged in a large series of collisions.[1] For example, in the scattering of a particle by a chain of atoms, the width of the wave packet decreases with increasing particle energy, and this makes the use of classical mechanics valid for relativistic particles.[1]

In evaluating the adequacy of the classical description, it is necessary to take into account another consideration. In channeling, particles execute finite motion in the transverse direction, and their transverse energies are quantized. The distance between levels for positively charged particles in the field of a planar channel, assuming that it is harmonic (see below), is $\Delta E_x = \hbar\omega$, where ω is the oscillation frequency. For the number of levels in a channel potential well of depth U_0 we have[21]

$$n^+ = U_0/\Delta E_x = \frac{d_p}{\hbar\sqrt{8}}\sqrt{U_0 m\gamma},$$

where d_p is the distance between planes, and m and γ are the mass and relativistic factor of the particle. When the number of levels is large and the transverse de Broglie wavelength of the particle is much smaller than the channel width, the quantized tunneling of particles to the sub-barrier region can be neglected. Therefore, the classical approach is completely justified, $n^+ \gg 1$, for heavy relativistic particles, and also for positrons (electrons) with energies above ~ 100 MeV.

2.1. The continuous-potential approximation

The motion of particles in a crystal at small angles to the atomic planes is described in a first approximation by a continuous planar potential[1] possessing translational symmetry in the transverse direction:

$$Y(x) = \sum_{n=-\infty}^{\infty} Y_1(x - nd_p), \tag{2}$$

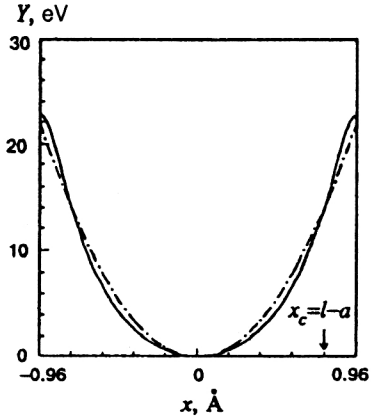

FIG. 2. Averaged potential of the (110) planar channel of a silicon crystal at room temperature in the Molière approximation for the atomic potential. The dashed line is the parabola approximation for the potential.

$$Y_1(x)=2\pi N d_p\int_0^\infty V(\sqrt{x^2+r^2})r\,dr, \tag{3}$$

where $Y_1(x)$ is the potential of an individual plane, averaged over the atom locations, assuming that the atoms are uniformly distributed, and N is the bulk density of atoms.

A one-dimensional periodic continuous potential of the set of atomic planes can also be obtained by expanding the three-dimensional periodic potential of the crystal in a Fourier series:[22]

$$V(\mathbf{R})=\sum_{k_x,k_y=k_z=0} V_{k_x}e^{ik_xx}+\sum_{k_y,k_z\neq 0} e^{ik_yy+ik_zz}$$

$$\times\sum_{k_x} V_{\mathbf{k}}e^{ik_xx}=Y(x)+W(\mathbf{R}). \tag{4}$$

Here $V_{\mathbf{k}}$ are the Fourier components of the crystal potential, and the term $W(\mathbf{R})$ includes the deviation of the full potential from the potential averaged along the planes. When the Molière atomic potential is used, the continuous potential of the set of planes takes the form[23]

$$Y(x)=2\pi Z_1Z_2e^2Nd_p\sum_{i=1}^{3}\frac{\alpha_i}{\kappa_i}\frac{\cosh[\kappa_i(x-d_p/2)]}{\sinh(\kappa_i d_p/2)}, \tag{5}$$

where $\kappa_i=\beta_i/a$. In Fig. 2 we show the potential of the (110) planar channel of a silicon crystal obtained by averaging (5) over the thermal oscillations of the atoms at room temperature.

Simpler model potentials are used in analytic calculations of the characteristics of particles channeled in a crystal. For example, in the channeling of positively charged particles, the potential of a planar channel at a distance from the channel walls larger than the amplitude of the atomic thermal oscillations is approximated well by a parabola (see Fig. 2):

$$U(x)=U_0(x/x_c)^2, \tag{6}$$

where $U_0=Y(a)$, $x_c=l-a$, $l=d_p/2$ is the half-width of the planar channel, and a is the screening length; for a completely ionized incident particle, $a=0.8853a_0Z_2^{-1/3}$, where $a_0=0.529$ Å is the Bohr radius.

Lindhard introduced the concept of critical approach of a particle to a row or plane of atoms, which limits the region of applicability of the continuous-potential approximation. For high-energy particles the averaged potentials of the chains and planes largely determine the behavior also in above-barrier states. The concept of the distance of critical approach in this case is used to determine the stability region of the channeled particle states. It is determined by the size of the region with increased nuclear density and is proportional to the amplitude u_1 of the atomic thermal oscillations. As shown by experiment[24] and by computer modeling,[25] a good estimate for silicon is $r_c\simeq 2.5u_1\simeq a$.

2.2. The equation of motion. Fundamental characteristics

The equation of motion of a relativistic particle in a crystal in the direction transverse to the planes has the following form in the continuous-potential approximation:

$$\frac{dp_x}{dt}=-\frac{dY(x)}{dx}. \tag{7}$$

The motion of the particles along the planes is free, and the corresponding momentum projections p_y and p_z are integrals of the motion, just like the total particle energy $W=m\gamma c^2+Y(x)$. The variation of the relativistic factor in the transverse particle motion can be neglected, and the equation of motion reduces to the nonrelativistic Newton equation with the particle mass equal to the relativistic mass:

$$m\gamma\ddot{x}=-Y'(x), \tag{8}$$

i.e., the transverse energy of the particle

$$E_x=\frac{m\gamma}{2}v_x^2+Y(x)=E^*\vartheta_x^2+Y(x) \tag{9}$$

is an integral of the motion. Here $v_x=v\vartheta_x$, ϑ_x is the angle that the particle momentum makes with the planes, and $E^*=pv/2\simeq E/2$.

If $E_x<Y_0$, where $Y_0\equiv Y(0)$ is the depth of the channel potential well, the x motion of a particle is finite. It is bounded by two adjacent planes, between which the particle oscillates. For $E_x>Y_0$ the x motion of the particles is infinite. Particles undergoing finite motion are called channeled, and ones undergoing infinite motion are called super-barrier or quasichanneled.

For orientation at an angle ϑ_{x0} relative to the planes at the entrance to the crystal, a particle crossing the entrance face at x_0 acquires an additional transverse energy due to the planar potential:

$$E_x(z=-0)=E^*\vartheta_{x0}^2\to E_{x0}\equiv E_x(z=+0)=E^*\vartheta_{x0}^2+Y(x_0). \tag{10}$$

At zero angle of incidence $E_{x0}=Y(x_0)\leqslant Y_0$, and practically all particles are captured into bound states by planar channels. At angles of incidence on the crystal $\vartheta_{x0}\geqslant\vartheta_c$, where ϑ_c is given by $E^*\vartheta_x^2=Y_0$, for all particles $E_{x0}\geqslant Y_0$, i.e., all particles are super-barrier. The angle

$$\vartheta_c=(Y_0/E^*)^{1/2}\simeq(2Y_0/E)^{1/2} \tag{11}$$

is known as the Lindhard critical channeling angle. For the (110) channel of silicon at room temperature, $Y_0=22.7$ eV, and the corresponding critical channeling angle for relativistic protons is

$$\vartheta_c[\mu\text{rad}]=6.74/\sqrt{p[\text{TeV}/c]}. \tag{11a}$$

Another commonly used definition of the critical angle is obtained by considering not the depth of the potential well of the planar channel, but the transverse energy $E_{xc}=Y(r_c)$ critical for the existence of stable trajectories of the channeled particles. For $r_c=2.5u_1$ we have $E_{xc}=14$ eV, and the corresponding critical angle is

$$\vartheta_c[\mu\text{rad}]=5.3/\sqrt{p[\text{TeV}/c]}. \tag{11b}$$

In the parabolic approximation for the planar-channel potential, a particle undergoes harmonic motion in the transverse plane,

$$x(t)=x_m \sin(\omega t+\varphi_0), \tag{12}$$

where x_m and φ_0 are the amplitude and initial phase of the oscillations, and $\omega=c\vartheta_c/x_c$ is the oscillation frequency. The longitudinal velocity in the approximation $\gamma=\text{const}$ varies as

$$v_z=\sqrt{v^2-v_x^2}\simeq v\left[1-\frac{1}{2}\left(\frac{\beta_m}{\beta}\right)^2\cos^2\omega t\right]. \tag{13}$$

The longitudinal position of the particle oscillates about the average value $\bar{z}=\bar{v}t$ with twice the frequency:

$$z(t)=\bar{\beta}ct-\Delta z_m \sin(2\omega t),$$

$$\bar{\beta}=\beta\left[1-\frac{1}{4}\left(\frac{\beta_m}{\beta}\right)^2\right],\quad \Delta z_m=\frac{v}{8\omega}\left(\frac{\beta_m}{\beta}\right)^2,$$

$$\beta_m=\frac{x_m\omega}{c},\quad \frac{\beta_m}{\beta}=\frac{x_m}{l}\vartheta_c. \tag{14}$$

The corresponding spatial period of the particle oscillations in the channel is

$$\lambda\equiv z(t=T)=\frac{\pi d_p}{\vartheta_c}\left[1-\frac{1}{4}\left(\frac{\beta_m}{\beta}\right)^2\right]\simeq\frac{\pi d_p}{\vartheta_c}, \tag{15}$$

which for protons in the (110) plane of silicon is

$$\lambda[\mu\text{m}]=114\sqrt{p[\text{TeV}/c]}. \tag{15a}$$

The probability of particle capture into the channeling regime for arbitrary angular distribution of the beam incident on the crystal $P(\vartheta_{x0})$ and uniform distribution of the coordinates x_0 of the points where particles enter the channel $P(x_0)=1/d_p$ is defined as

$$P_c^0=\frac{2}{d_p}\int_{r_c}^{d_p-r_c}dx_0\int_0^{\vartheta_c(x_0)}P(\vartheta_{x0})d\vartheta_{x0},$$

$$\vartheta_c(x_0)=\left(\frac{E_{xc}-Y(x_0)}{E^*}\right)^{1/2}. \tag{16}$$

For a beam with Gaussian angular distribution

$$P_c^0=\frac{2}{d_p}\int_{r_c}^{l}Erf[\tilde{\vartheta}_c(x_0)]dx_0,\quad \tilde{\vartheta}_c(x_0)=\frac{\vartheta_c(x_0)}{\sqrt{2}\bar{\vartheta}_x}, \tag{16a}$$

where $\bar{\vartheta}_x$ is the rms deviation. For a uniform distribution of beam particles in the angular range $(-\Phi,\Phi)$, the capture probability is determined by the ratio of the phase space of the channeling in the space (x,ϑ_x), i.e., the area $S=\pi x_c\vartheta_c$ of the phase ellipse of a channeled particle with $E_x=E_{xc}$, to the total phase space of the beam $2\Phi d_p$:

$$P_c^0=\frac{\pi x_c\vartheta_c}{2\Phi d_p}=\frac{\pi\vartheta_c}{4\Phi}(1-r_c/l). \tag{16b}$$

For a unidirectional beam of particles entering the crystal parallel to the planes, the capture probability is simply determined by the ratio of the useful channel width d_p-2r_c to the total width:

$$P_c^0=1-r_c/l. \tag{16c}$$

3. CHANNELING IN A BENT CRYSTAL

3.1. The main features

The equation of motion of fast charged particles channeled in bent channels of a crystal lattice was first studied in Ref. 26 in connection with study of particle dechanneling at dislocations. A crystal bending which can be realized in practice always satisfies the condition $R\gg d_p$, where R is the bend radius; i.e., a centrifugal force $F_c=pv/R$ of constant magnitude acts on the channeled particle everywhere in the cross section of the bent channel. Therefore, the equation of motion of a particle in a bent crystal has the form

$$x''+\frac{1}{pv}Y'(x)=k, \tag{17}$$

where $k=1/R$. In the parabolic approximation for the channel potential the solution of the equation

$$x''+\bar{\omega}^2x=k \tag{17a}$$

is a harmonic oscillator whose equilibrium spectrum is shifted toward the bend radius by $x_0=k/\bar{\omega}^2$, where $\bar{\omega}=\vartheta_c/x_c$.

In Ref. 27 the fraction of particles entrained by the crystal bend was analyzed by introducing an effective potential with the additional centrifugal term acting on a particle in a bent crystal:

$$Y_{\text{eff}}(x,R)=Y(x)\pm\frac{pv}{R}x+Y_{c0}(R). \tag{18}$$

The sign of the centrifugal term depends on the direction in which the transverse coordinate x is measured; if the latter is toward the bend radius vector it is minus, otherwise it is plus. The constant term Y_{c0} is chosen such that the effective potential is zero at the minimum. The effective potential of a bent planar crystal is shown in Fig. 3.

In the harmonic approximation for the planar-channel potential (6), the effective potential can be written as

$$U_{\text{eff}}(x,R)=U_0\left(\frac{x-x_0}{x_c}\right)^2,\quad x_0=\frac{E^*}{U_0}\frac{x_c^2}{R}=\frac{F_c}{2U_0}x_c^2. \tag{19}$$

Here U_0 denotes the critical transverse channeling energy in a straight crystal, $U_0=Y(r_c)$. When the crystal is bent, the

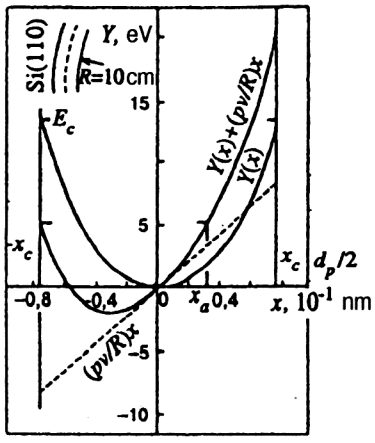

FIG. 3. Effective potential of the (110) channel of a silicon crystal bent with radius 10 cm for 10-GeV protons.

minimum of the effective potential is shifted to the outer wall of the channel by a distance x_0, which leads to the corresponding shift of the channeled-particle trajectories. At the same time the potential barrier separating adjacent planar channels is lowered. The critical transverse channeling energy is therefore decreased:[28,29]

$$E_{xc}(F_c)=U_{\text{eff}}(x_c,F_c)=U_0(1-x_0(F_c)/x_c)^2. \quad (20)$$

The critical bend radius of planar channels R_c can be defined as the radius at which the minimum of the effective potential reaches the boundary of the stability region x_c:

$$x_0(R_c,E)=x_c \rightarrow R_c(E)=x_c\frac{E^*}{U_0}. \quad (21)$$

Along with R_c, there is a critical particle energy E_c for channeling in a crystal with a given bend radius:[28,29]

$$x_0(R,E_c)=x_c \rightarrow E_c^*=U_0\frac{R}{x_c}. \quad (22)$$

The critical transverse energy in a straight crystal is practically independent of the particle energy. In a bent crystal it decreases with increasing particle energy, owing to the increase of the centrifugal force. The dependence of E_{xc} on R and E in a bent crystal can be written as

$$E_{xc}(R)=U_0(1-R_c/R)^2, \quad E_{xc}(E)=U_0(1-E/E_c)^2. \quad (23)$$

The critical channel angle changes accordingly:

$$\vartheta_c(R)=\vartheta_c^0(1-R_c/R), \quad \vartheta_c(E)=\vartheta_c^0(E)(1-E/E_c), \quad (24)$$

where $\vartheta_c^0=(2U_0/E)^{1/2}$ is the value in a straight crystal.

The decrease of the critical channeling angle and the shift of the trajectories toward the channel wall as the crystal is bent tend to decrease the probability for particle capture in the channeling regime. For a parallel beam of particles entering the bent planes tangentially, the capture is reduced, owing to the decreased channel cross section $2(x_c-x_0)$ where stable trajectories of the channeled particles can be realized. For the capture probability we have

$$P_c(R)=P_c^0(1-R_c/R), \quad P_c(E)=P_c^0(1-E/E_c). \quad (25)$$

The dependence of the particle capture probability in the planar channeling regime by the (110) channel of silicon on the bend radius of the crystal and on the particle energy is shown in Fig. 4. The capture probability decreases rapidly for $R<10R_c$ (Fig. 4a). In a bent crystal the capture falls off with increasing particle energy, and the more strongly bent the crystal, the more rapidly this occurs (Fig. 4b). For a broad beam with uniform angular distribution of the particles, the dependence of the capture probability on R and E will be stronger:[30]

$$P_c(R)=P_c^0(1-R_c/R)^2, \quad P_c(E)=P_c^0(E)(1-E/E_c)^2. \quad (25a)$$

Therefore, when the crystal is bent, a strong dependence of the basic channeling characteristics on the particle energy appears.[29]

3.2. The equation for the particle trajectory

In the approximation of continuous potential of the atomic planes, the passage of quasichanneled particles through a crystal bent with constant radius is equivalent to scattering by the part of the axially symmetric electric field possessing radial periodicity.[31] Assuming for simplicity that the particle velocity along the field axis (the crystal bending axis) is zero, the equations of motion of a relativistic particle in the axially symmetric field of a bent crystal in polar coordinates (r,φ) are

$$\frac{d}{dt}(m\gamma\dot{r})=m\gamma r\dot{\varphi}^2-\frac{dU}{dr}, \quad (26)$$

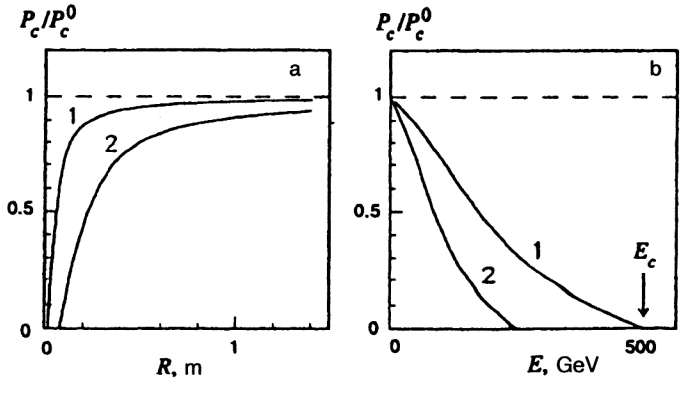

FIG. 4. Dependence of the probability for proton capture into the channeling regime by the (110) channel of silicon (a) on the bend radius R of the crystal for (1) 10-GeV and (2) 40-GeV protons, and (b) on the proton energy E in a crystal bent with radius (1) 100 cm and (2) 50 cm.

$$\frac{d}{dt}(m\gamma r^2\dot{\varphi})=0, \tag{27}$$

$$\frac{d}{dt}(m\gamma c^2)=-\dot{r}\frac{dU}{dr}. \tag{28}$$

The total energy and angular momentum of the particle relative to the center of the field are integrals of the motion:

$$W=m\gamma c^2+U(r), \tag{29}$$

$$M=m\gamma r^2\dot{\varphi}. \tag{30}$$

From the integrals of the motion we find the equation for the particle trajectory:

$$\varphi(r)=\pm M\int\frac{r^{-2}dr}{[(W-U(r))^2/c^2-M^2/r^2-m^2c^2]^{1/2}}+\varphi_0, \tag{31}$$

where φ_0 is a constant. The integrals of the motion W and M are determined by the initial conditions $(\mathbf{r}_0,\mathbf{v}_0)$ under which the particle enters the crystal:

$$W=E_0+U(r_0),\quad M=m\gamma_0|[\mathbf{rv}]|=r_0E_0\beta_0c^{-1}\cos\vartheta_0,$$

where $E_0=m\gamma_0c^2$, $\beta_0=v_0/c$, and ϑ_0 is the angle between the particle momentum $\mathbf{p}_0$ and the direction of the tangent relative to the bent planes at the entrance to the crystal. For a crystal whose size in the radial direction Δr is much smaller than the bend radius, $\Delta r\ll R_0$ (measuring the radial coordinate r from the point with bend radius R_0) and for high-energy particles $(E_0\gg U(r))$, we have[31]

$$\varphi(r)=\frac{\sqrt{E^*}}{R_0}\cos\vartheta_0 \times\int_{r_0}^{r}\frac{dr}{\left[E^*\sin^2\vartheta_0+\frac{2E^*}{R_0}(r-r_0)-(U(r)-U(r_0))\right]^{1/2}}. \tag{32}$$

We therefore arrive at the approximation commonly used to study particle channeling in a bent crystal. According to it, the bending of the crystal is taken into account by the introduction of a constant centrifugal force $F_c=2E^*/R_0$ and an effective potential acting on the particle:

$$U_{\text{eff}}(r,R_0)=U(r)-\frac{2E^*}{R_0}r. \tag{33}$$

Here the transverse (radial) energy of the particle $E_r=E^*\sin^2\vartheta_0+U_{\text{eff}}(r,R_0)$ is an integral of the motion. Characterizing the crystal bending by the centrifugal force F_c acting on the particle and measuring the angles in units of the critical angle $\vartheta_c=(U_0/E^*)^{1/2}$, we arrive at the equation for the particle trajectory in a form independent of the particle energy:

$$\bar{\varphi}(r,F_c)=\frac{F_c}{2U_0^{1/2}}\int_{r_0}^{r}\times\frac{dr}{[U_0\bar{\vartheta}_0^2+U_{\text{eff}}(r_0,F_c)-U_{\text{eff}}(r,F_c)]^{1/2}}, \tag{34}$$

where $\bar{\varphi}=\varphi/\vartheta_c$ and $\bar{\vartheta}_0=\vartheta_0/\vartheta_c$.

3.3. Dechanneling in a bent crystal

3.3.1. The kinetic equation

In the approximation of continuous potential of the atomic rows and planes, the particle transverse energy is an integral of the motion. However, the difference between the real potential of a crystal and the continuous potential, the term $W(\mathbf{R})$ in Eq. (4), and also scattering on electrons and crystal defects tend to change the transverse energy of the particles and dechannel them. The defect concentration is very small in the semiconductor crystals of silicon and germanium commonly used in channeling experiments. The contribution to dechanneling from catastrophic collisions with the crystal electrons, which lead to scattering at angles larger than the critical channeling angle, is small. Particle dechanneling occurs as a result of multiple scattering on electrons and nuclei with a gradual change of the particle transverse energy. The evolution of the change of the channeled-particle density in phase space near E_x due to multiple scattering is described by the Fokker–Planck equation:

$$\frac{\partial f}{\partial z}=-\frac{\partial}{\partial E_x}(Af)+\frac{\partial^2}{\partial E_x^2}(Bf). \tag{35}$$

In the definition of the diffusion coefficients A and B, there is an average over the cross sections of the corresponding processes (electron and nuclear scattering) and the equilibrium distribution of the channeled particles in the crystal $P_0(E_x,x)$ (Ref. 1):

$$P_0(E_x,x)=\begin{cases}2/[T(E_x)\dot{x}(E_x,x)], & E_x>U(x),\\ 0, & E_x<U(x),\end{cases}$$

$$\dot{x}(E_x,x)=c[2(E_x-U(x))/E]^{1/2}, \tag{36}$$

where $T(E_x)$ is the period of oscillation of a particle in the channel.

After the averaging, the friction and diffusion coefficients of the channeled particles have the form

$$A(E_x)=\langle E\overline{\eta_z^2}\rangle, \tag{37}$$

$$B(E_x)=\langle 2(E_x-U(x))E\overline{\eta_z^2}\rangle+\left\langle\frac{1}{2}E^2\overline{\eta_z^4}\right\rangle, \tag{38}$$

where $\eta=\theta\cos\varphi$ is the projection of the scattering angle θ on the x axis, and the subscript z indicates that the quantities in question pertain to unit path along z. The second term in the diffusion coefficient can be neglected for transverse particle energies which are not too small, which gives the relation between the diffusion coefficients:[32]

$$TA(E_x)=\frac{\partial}{\partial E_x}TB(E_x). \tag{39}$$

Equation (39) transforms the Fokker–Planck equation into a diffusion type of equation:

$$\frac{\partial f}{\partial z}=\frac{\partial}{\partial E_x}\left[BT\frac{\partial}{\partial E_x}\left(\frac{f}{T}\right)\right]=AT\frac{\partial}{\partial E_x}\left(\frac{f}{T}\right)+BT\frac{\partial^2}{\partial E_x^2}\left(\frac{f}{T}\right). \tag{40}$$

The first term in the equation leads to monotonic growth of the transverse energy of the channeled particles owing to multiple scattering and gives a good description of the behavior of particles with large transverse energies. For particles with small transverse energies the diffusion described by the second term is important.

In a straight crystal, dechanneled particles, which remain for some time near the capture angular range, can again be captured into the channeling regime as a result of strong multiple scattering on nuclei in crossing the atomic planes.[33] However, in a bent crystal, owing to the bending of the planar channels, dechanneled particles rapidly leave the capture region and, as shown by the results of modeling,[33] there is practically no recapture. This fully justifies the use of the boundary condition

$$f(E_{xc},z)=0, \tag{41}$$

which excludes exchange between the channeled and quasi-channeled fractions of the beam, in solving Eq. (40).

The equation becomes simpler in the harmonic approximation for the planar-channel potential, when the particle oscillation period in the channel does not depend on the particle transverse energy:

$$\frac{\partial f}{\partial z}=\frac{\partial}{\partial E_x}\left[B\frac{\partial f}{\partial E_x}\right]. \tag{42}$$

The solution of this equation with diffusion coefficient $B(E_x)=B_0E_x^{\alpha}$ for the boundary condition (41) and the initial condition

$$f(E_x,0)=F_0(E_x), \tag{43}$$

where $F_0(E_x)$ is the initial transverse-energy distribution of the channeled particles, was obtained in Ref. 34. Then the dependence of the fraction of channeled particles on the beam penetration depth in the crystal is found to be[28]

$$F_{ch}(z)=\int_0^{E_{xc}}f(E_x,z)dE_x=\sum_{n=1}^{\infty}q_n\exp(-z/\lambda_n),$$

$$\lambda_n=\left(\frac{2}{2-\alpha}\right)^2\mu_{\nu,n}^{-2}\frac{E_{xc}^{2-\alpha}}{B_0}, \tag{44}$$

where $\mu_{\nu,n}$ are the zeros of the Bessel function J_{ν}. Since the damping length of the nth term of the expansion is $\lambda_n\propto 1/\mu_n^2$ and decreases rapidly with n, for penetration depths $z>\lambda_2$ the fraction of channeled particles is primarily determined by the first term and falls off exponentially. Experimental studies[24] and numerical experiments on the deflection of a beam by a bent crystal[33] also indicate exponential decrease of the number of channeled particles with penetration depth in the crystal. Therefore, for the dechanneling length at $\alpha=1$ we have

$$z_{1/e}\simeq\lambda_1=\frac{4E_{xc}}{\mu_{0,1}^2A}. \tag{45}$$

This value is independent of the initial transverse-energy distribution of the particles at the entrance to the crystal.

As noted above, when the crystal is bent the trajectories of the channeled particles are shifted toward the outer wall of the channel. As a result, particles with a given transverse energy moving through a region with higher density of electrons and nuclei undergo stronger scattering than in a straight crystal. Moreover, when the crystal is bent the critical transverse channeling energy is decreased. Both of these factors tend to decrease the channeling lengths for a bent crystal. The features of the dechanneling in a uniformly bent crystal were first studied in Refs. 28 and 29.

3.3.2. The role of lowering of the potential barrier

In bending of a crystal far from the critical value, a source of dechanneling is multiple scattering on electrons, the density of which in the central part of a planar channel for a silicon crystal is primarily determined by the valence electrons. Approximating the valence-electron density as constant along the channel, $\rho_v=NZ_v$, the electron friction coefficient is independent of the transverse energy E_x of a channeled proton, and the diffusion coefficient depends linearly on E_x:

$$A=E^*\overline{\eta_z^2},\quad B=AE_x, \tag{46}$$

i.e., in the power-law approximation we have the diffusion coefficient $B_0=A$ and $\alpha=1$, and Eq. (45) is valid for the dechanneling length. The mean squared angle of proton scattering on electrons of the crystal

$$\overline{\eta^2}=\frac{e^4}{E^{*2}b_{\max}^2}\ln(b_{\max}/b_{\min}) \tag{47}$$

can be estimated as in Ref. 35. The maximum impact parameter of a collision $b_{\max}$ is determined from the condition that the momentum transferred to an electron of the crystal be sufficient to ionize (excite) the outer electrons of the atom:

$$\Delta p=\frac{2e^2}{vb}\geqslant\frac{\hbar}{r_a},\quad b_{\max}=2r_a\alpha/\beta, \tag{48}$$

where $\alpha=e^2/\hbar c$, r_a is the atomic radius, and the minimum impact parameter $b_{\min}$ is found from the condition $\theta(b_{\min})=\theta_c$:

$$b_{\min}=\frac{e^2}{\vartheta_cE^*}=\frac{e^2}{\sqrt{E_{xc}E^*}}, \tag{49}$$

dividing the region of multiple collisions from the region of single collisions with electrons of the crystal in the dechanneling process.

For the dechanneling length in a straight crystal $S_{1/e}^o$ we have

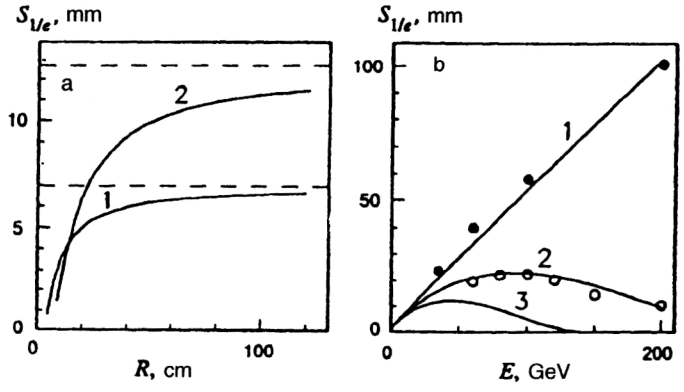

FIG. 5. Dependence of the dechanneling length in the (110) channel of silicon (a) on the bend radius R of the crystal for (1) 10-GeV and (2) 20-GeV protons, and (b) on the proton energy E in (1) a straight crystal and in a crystal bent with radius (2) 80 cm and (3) 40 cm. The dashed lines are for a straight crystal, and the points are from the Fermilab experiment.

$$S^0_{1/e}=k_1E^*/\ln(k_2\sqrt{E}), \tag{50}$$

$$k_1=\frac{4}{\mu^2_{0,1}}\frac{E_{xc}}{NZ_v\pi e^4}, \quad k_2=\sqrt{2}\alpha\frac{r_a\sqrt{E_{xc}}}{e^2}.$$

If we use $E_{xc}=14$ eV for the (110) channels of silicon, the dechanneling lengths calculated from (50) agree to within 15% with the experimentally measured values.[36]

In this approximation, the change of the dechanneling length when the crystal is bent is determined by the change of the critical transverse channeling energy E_{xc}:

$$S_{1/e}(R)=S^0_{1/e}(1-R_c/R)^2. \tag{51}$$

In Fig. 5a we show the dechanneling lengths, calculated from (50) and (51), of 10 and 20 GeV protons in the (110) channel of a silicon crystal as functions of the channel bend radius. The dechanneling length decreases sharply upon bending, which leads to a significant decrease of E_{xc}, i.e., for $R\leqslant 10R_c$.

In Fig. 5b we show the calculated dependence of the proton dechanneling length in the (110) channel of silicon on the particle energy. In a straight crystal the dechanneling length grows roughly linearly with the particle energy, because the coefficient of friction behaves as $A\sim 1/E$ (curve 1). In this figure we also show the experimental results.[36] We see that the approximation $\rho=\rho_v$ satisfactorily describes experiment. The strong dependence of the critical transverse energy E_{xc} on the particle energy in a bent crystal radically changes the E dependence of the dechanneling lengths:[28,29]

$$S_{1/e}(E)=S^0_{1/e}(E)[1-E/E_c]^2, \tag{52}$$

spoiling the proportionality (curves 2 and 3). Beginning at a certain proton energy $E_m(R)$, the decrease of the coefficient of friction A with increasing particle energy ceases to compensate for the decrease of E_{xc} in a bent channel. Consequently, the dechanneling length has a maximum at E_m and then decreases to zero when the proton energy reaches the critical value $E_c(R)$ for channeling in a bent crystal.

In the first experiment performed at Dubna on the deflection of 8.4-GeV protons by a silicon crystal bent along the (111) channels, the bend radius of the crystal was more than 20 times greater than the critical radius, and so there was no significant change of the dechanneling length. According to the experimental results, the dechanneling length was 0.82 cm. An estimate using the approximation $\rho=\rho_v$ =const gives $S_{1/e}=0.7$ cm. However, it should be noted that the measurements were performed on a segment of crystal with decreasing curvature, where the dechanneling lengths should be observed to increase (see below). A later experiment at Fermilab at higher particle energies[24] and uniform bending of the crystal fully confirmed the behavior of the dechanneling length as a function of the particle energy predicted in Ref. 28 (experimental points near curve 2 in Fig. 5b).

3.3.3. The change in the multiple scattering

For strong bending of the crystal, the channeled-particle trajectories are significantly shifted toward the outer wall of the channel, and the model of constant electron density cannot describe the resulting increase of multiple scattering on electrons of the crystal, in which an increasingly important role is played by the core electrons, the density of which increases markedly as the channel walls are approached. To correctly determine the proton dechanneling lengths in this case it is necessary to take into account the distribution of the electron density over the channel cross section and multiple scattering on nuclei.

In Ref. 28 it was shown how the electron and nuclear diffusion coefficients change as the crystal is bent. In a straight crystal nuclear scattering is important only at the periphery of the channel for particles with large transverse energy. As the bending of the crystal increases, the nuclear diffusion coefficient grows for fixed transverse energy of the particles, and at sufficiently strong bending with $R\simeq 2R_c$ it becomes close in value to the electron diffusion coefficient. Therefore, for strong bending of the crystal the dechanneling lengths are largely determined by nuclear scattering, in contrast to the case of a straight crystal.[28] This leads to a strong temperature dependence of the dechanneling lengths in a strongly bent crystal, which was subsequently discovered experimentally.[24]

3.3.4. Bend dechanneling

In a crystal which is bent nonuniformly, on a segment with increasing curvature or in going from a straight to a bent part of the crystal, a significant fraction of the beam is ejected from the channeling regime, owing to a mechanism unrelated to multiple scattering: centrifugal or bend dechanneling.[37–39] In going from a straight to a uniformly

bent part of the crystal, particle knockout from the channeling regime occurs at distances smaller than the oscillation length λ of the particles in the channel. The fate of a particle in this transition, neglecting the insignificant multiple scattering, is uniquely determined by its entrance parameters.

In the 3- or 4-point bending devices used in the first experiments on deflecting charged-particle beams, the curvature of the bend varied over the entire length of the bent part of the crystal. For example, in a three-point bender the bend curvature increases roughly linearly in approaching the center of the crystal. In this case, centrifugal dechanneling occurs over the entire crystal segment with increasing curvature, the length of which is considerably larger than λ, i.e., the process is lengthy owing to the gradual decrease of the depth of the effective potential well and the shift of the particle trajectories toward the outer wall of the channel.

The dependence of the fraction of particles dechanneled owing to the centrifugal mechanism on a crystal segment with increasing curvature was obtained in Ref. 40. In the harmonic approximation for the channel potential $U(x) = \alpha x^2/2$ the solution of the equation of motion

$$\frac{d^2x}{dz^2} + \frac{1}{pv} U'(x) = \kappa(z) \tag{53}$$

on a segment whose curvature grows linearly, $\kappa(z) = \kappa_0 z$, has the form

$$x(z) = x_m \cos(\bar{\omega} z + \phi_0) + (\kappa_0/\omega^2) z, \tag{54}$$

where $\bar{\omega}^2 = \alpha/pv$. The second term describes the shift of the equilibrium orbit, which increases with z, owing to the increase of the channel curvature. A particle is dechanneled for $x_m + (\kappa_0/\bar{\omega}^2) z \geq l$. The fraction of dechanneled particles increases linearly with depth:

$$F_d(z) = \frac{\kappa_0}{l\bar{\omega}^2} z. \tag{55}$$

Of course, along with centrifugal dechanneling on a segment with increasing curvature, the usual dechanneling mechanism due to multiple scattering is also operating.

In cases which can be realized in practice, the change of curvature of a crystal over the oscillation length of the channeled particles is small, so that motion of the particles in an effective potential whose parameters vary adiabatically slowly can be studied. The drift of the particle transverse energy associated with the change of curvature is described by the coefficient[21]

$$A_c = \left\langle \frac{\Delta E_x}{\Delta z} \right\rangle_c = k'(\langle x \rangle + x_c), \tag{56}$$

where $\langle x \rangle$ is the coordinate of the channeled particle averaged over a period, $k' = dk/dz$, and $k = pv/R(z)$. For constant curvature of the crystal the dechanneling length is determined in terms of the electron coefficient of friction A_e (45). For nonuniform bending, the drift of the transverse energy is due both to multiple scattering on the crystal electrons, and to the change of curvature of the crystal:

$$A = A_e + A_c. \tag{57}$$

Neglecting diffusion in multiple scattering, the dechanneling length in a nonuniformly bent crystal can be estimated as[21]

$$S_d(k' \neq 0) \sim \frac{S_d^{R=\text{const}}}{1 + A_c/A_e}. \tag{58}$$

For increasing curvature of the crystal, when k', $A_c > 0$, the dechanneling length becomes smaller than in a uniformly bent crystal $S_d^{R=\text{const}}$, owing to the additional centrifugal drift mechanism.

3.3.5. The effect of decreasing curvature on dechanneling

Nonuniformity of the crystal bending can also lead to the opposite effect. On a segment with decreasing curvature, when k', $A_c < 0$, increase of the depth of the effective potential well of the planar channels along the crystal causes the transverse particle energy to drift, which slows the growth of E_x due to multiple scattering. As a result, the dechanneling length becomes larger than in a uniformly bent crystal (58).

This increase of the dechanneling length has been discovered experimentally.[41] For example, the dechanneling length of 100-GeV protons in a straight silicon crystal along the (110) direction is about 60 mm (Ref. 36), while along the (111) direction in a bent crystal on a segment with decreasing curvature it is 100 mm (Ref. 41). Although the experimental results were obtained for different crystal orientations, the observed difference in the dechanneling lengths was much larger than expected, about 20%, and is associated with the gradient mechanism which "deepens" the transverse energy levels of channeled particles for decreasing channel curvature. A very large effect was observed for 60-GeV protons, for which the dechanneling length on a segment with decreasing curvature was more than three times its value in a straight crystal.

3.3.6. The angular unfolding of dechanneling

Particles ejected from the channeling regime in the bent part of a crystal at some value of the longitudinal coordinate z are deflected by an angle

$$\vartheta(z) = \int_0^z \kappa(z')dz'. \tag{59}$$

The experimentally measured distributions of deflection angles allow the dependence $F_d(z)$ to be reconstructed accurately. This angular unfolding of the dechanneling process in a bent crystal, a "dechanneling spectrometer,"[12] provides a convenient tool for studying particle dechanneling.

In the experiment of Ref. 12 on the deflection of protons with energy of up to 180 GeV by a silicon crystal bent along the (111) planes, bend dechanneling was manifested very clearly, because the curvature of the crystal was close to the critical value at high energies. In Fig. 6 we show the deflection-angle distributions of 60-GeV protons obtained separately for the fractions of particles passing near the outer and inner faces of a bent crystal.

In addition to the maxima in the direction of the incident beam and at the bending angle, there is another maximum roughly in the center. It is formed by particles which leave

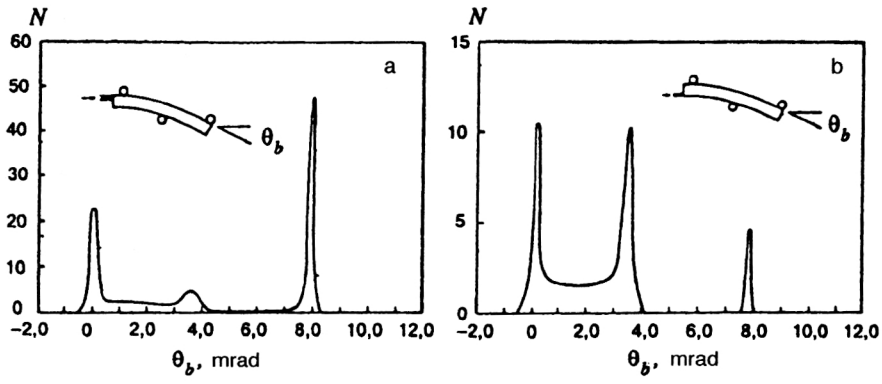

FIG. 6. Angular distribution of 60-GeV protons deflected by a silicon crystal bent along the (111) plane in a 3-point bending device, separately for the fractions of particles passing near the (a) outer and (b) inner faces of the crystal (results of a Fermilab experiment).

the channeling regime near the central support, and is manifested more strongly for particles passing through the crystal layer bordering the support. This is because, in addition to the change of the "global" curvature along the crystal when it is bent, there are local distortions of the crystal lattice at the three supports due to the support pressure. These are maximal for the crystal layers adjacent to the supports and gradually decrease in layers farther from the support. The strong local curvature of the crystal channels near the central support induces a centrifugal dechanneling of the particles, which significantly contributes to the formation of the central maximum in the angular distribution.

The maximum in the incident-beam direction is due to particles knocked out of the channeling regime, owing to multiple scattering in the straight part of the crystal and to centrifugal dechanneling near the forward support. Another distinguishing feature of the angular distributions is the presence of a large number of particles which are dechanneled in the forward bent part of the crystal and the near absence of such particles beyond the central support. The ejection of particles from the channeling regime in the forward part of the crystal with increasing global curvature of the channels is due to both centrifugal dechanneling and multiple scattering. Small losses of particles beyond the central support occur because the increasing depth of the potential well with decreasing channel curvature slows the process of particle ejection due to multiple scattering.

Multiple scattering contributes little to the formation of the central maximum, owing to the small extent of the crystal segment near the support with increased local curvature, so that here centrifugal dechanneling is manifested in its purest form. This fact has been used to measure the dependence of the fraction of particles dechanneled by the centrifugal mechanism on the bend force pv/R (Ref. 12).

3.4. The efficiency of beam deflection by a crystal

When bent crystals are used to steer beams of high-energy charged particles, it is useful to make preliminary estimates of the efficiency with which the beams can be deflected by the crystal. The efficiency of beam deflection by a uniformly bent crystal P_d was determined in Refs. 28 and 29. It was shown that there are optimal crystal parameters for deflecting a beam at a given angle.

The deflection efficiency is determined by the probability for particle capture into the channeling regime P_c and the probability for the particles to pass through the entire crystal in the channeling regime $P_{\rm ch}$. For example, for the efficiency of deflecting particles by a given angle α we have

$$P_d(\alpha,R)=P_c(R)\times P_{\rm ch}(\alpha,R), \tag{60}$$

$$P_{\rm ch}(\alpha,R)=\exp[-\alpha R/S_{1/e}(R)].$$

Rotation of the beam by an angle $\alpha=L/R$ can be achieved for various bend radii R and crystal lengths L.

In Fig. 7a we show the dependence of the efficiency of deflecting a parallel beam of 10-GeV protons by an angle of 20 mrad on the crystal bend radius R. We also show the dependences $P_c(R)$ and $P_{\rm ch}(R)$. The probability of "channeling" through the entire crystal is maximal for crystal bending with radius $R'_m\simeq 3R_c$. It is smaller for $R<R'_m$, owing to the large decrease of the dechanneling length, and for large R, owing to the increase of the crystal length required for deflection by an angle α. The beam deflection efficiency has a maximum at $R_m>R'_m$ owing to the strong dependence of the probability for capture into the channeling regime in the region $R<10R_c$.

The optimal bend radius of a crystal can be determined from (60) by using the condition $\partial P_d/\partial R=0$. When the reduced curvature $\rho=R_c/R$ is used as the variable, the deflection efficiency for a beam with uniform angular distribution takes the form[30]

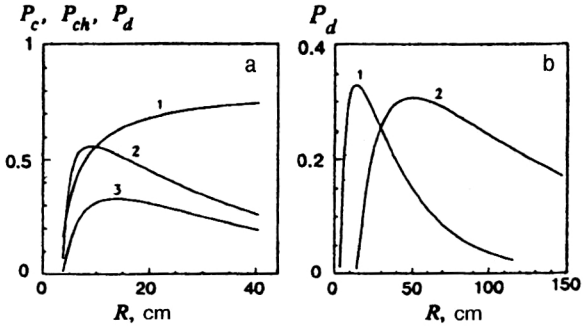

FIG. 7. (a) Dependence of (1) the probability for capture into the channeling regime, (2) the probability for passing through the entire crystal in the channeling regime, and (3) the efficiency of deflection by an angle of 20 mrad, for 10-GeV protons, on the bend radius of a silicon crystal bent along the (110) planes. (b) Comparison of the efficiency of deflection at an angle of 20 mrad for protons of energy (1) 10 GeV and (2) 40 GeV.

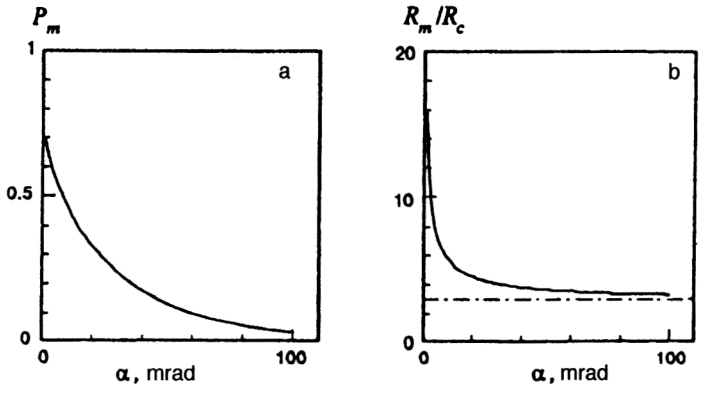

FIG. 8. Bending-angle dependence of (a) the maximum efficiency of deflection of a parallel beam of 10-GeV protons by a silicon crystal bent along the (110) planes, and (b) the optimal bending radius of the crystal.

$$P_d(\alpha,\rho)=P_c^0(1-\rho)^2\exp\left(-\frac{\alpha/\theta_D}{\rho(1-\rho)^2}\right), \tag{61}$$

and the equation determining the optimal bending is written as

$$\alpha/\theta_D=\frac{2\rho^2(1-\rho)^2}{1-3\rho}, \tag{62}$$

where the parameter $\theta_D=S^0_{1/e}/R_c$ characterizes a deflection angle close to the maximum possible one. Equation (62) leads to the bound $\rho_m>1/3$, i.e., the optimal bend radius is always greater than $3R_c$.

In Fig. 7b we compare the proton deflection efficiencies for two values of the particle energy. For the same effective crystal bend ρ the probability of capture into the channeling regime and localization of the channeled-particle trajectories in the cross section of the bent channel are identical. However, the weak E dependence remains, $\theta_D\sim 1/\ln(kE^{1/2})$, and so with increasing particle energy the change of scale in R is accompanied by slow decrease of the deflection efficiency.

It is natural to expect that increase of the deflection angle should decrease the efficiency of beam deflection by a crystal, since this requires an increase of the crystal length or bending, and both tend to enhance particle dechanneling. In Fig. 8a we show the dependence of the maximum efficiency of deflecting a parallel beam of 10-GeV protons by bent (110) planar channels of silicon on the value of the bending angle. The deflection efficiency falls off exponentially with increasing α. The α dependence of the optimal bend radius R_m is shown in Fig. 8b. For large angles $\alpha>0.01$ rad, strong bending of a crystal with $r<5$ is optimal, because any increase of R leads to an increase of the crystal length associated with the dechanneling length.

3.5. Efficiency of a crystal deflector

So far, only silicon crystals have been used as deflectors for splitting and extracting a beam from an accelerator. This is a consequence of the high quality of the single crystals now obtainable, with extremely low impurity content and practically no dislocations. In addition, a silicon crystal is a semiconductor and allows the design of intrinsic surface-barrier detectors, making the crystal a "live" target which gives information about the state of the particles passing through it on the basis of the ionization that they produce.

The use of crystals with higher atomic number, which have stronger intracrystalline fields, can significantly raise the efficiency of crystal deflectors. Recently, attempts have been made to use germanium crystals ($Z_2=32$) in experiments on proton-beam deflection.[9,10] In a CERN experiment using a 450-GeV proton beam, it was found that the deflection efficiency is increased in relation to that of a silicon deflector for large bending angles.

Thanks to the large amplitudes of thermal oscillations and its high melting temperature and radiation stability, tungsten ($Z_2=74$) is one of the best possible materials for use as a crystal deflector.[17] However, obtaining tungsten crystals of the required size with low dislocation density is a serious problem.[41]

The cross section for dechanneling on dislocations grows with the particle energy. Estimates including near and distant collisions of particles with dislocations show that use of the available tungsten crystals with dislocation density below 10^4 cm^{-2} can lead to a significant gain in deflection efficiency for beams of relativistic nuclei with energy of several GeV/nucleon. There is an ongoing project to study tungsten deflectors using the relativistic nuclear beam of the Nuclotron at the JINR.[42]

In Table I we give the principal parameters of (110) planar channels in silicon and tungsten crystals (for $r_c=2.5\,u_1$). The significant increase of the depth of the potential well and the electric field strength in tungsten lead to an increase of the critical channeling angles by more than a factor of two, while the critical bend radii are decreased by about a factor of seven. This allows stronger bending of the crystals and larger angular deflection of the beam for a given crystal length. The relatively small amplitudes of thermal oscillations of the atoms in tungsten ensure a large effective channel width, $A_s=1-2r_c/d_p$, which along with the increase of the channeling angles enhances the capture of particles into the channeling regime. Although the electron density in tungsten channels is higher, the dechanneling lengths

TABLE I. Parameters of (110) planar channels of silicon and tungsten crystals.

Crystal	d_p, Å	u_1, Å	A_s	U_0, eV	E_{xc}, eV	$\mathscr{E}_{\max}$, GV/cm
Si	1.92	0.075	0.8	22.7	14.32	5.97
W	2.238	0.05	0.89	131.9	91.61	42.52

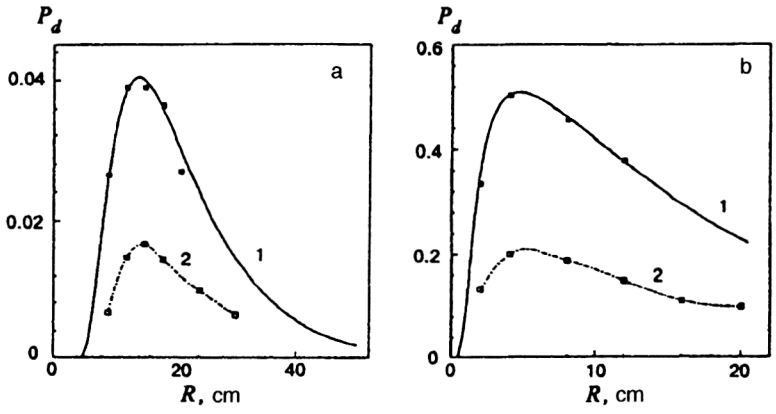

FIG. 9. Bending-angle dependence of the efficiency of deflecting $^{12}_{6}$C nuclei of energy 6 GeV/nucleon by crystals of (a) silicon and (b) tungsten, bent at an angle of 100 mrad along the (110) planes. (1) Parallel beam; (2) beam with uniform angular distribution in the range $(-\vartheta_c, \vartheta_c)$. The points are the results of modeling.

are longer than in silicon, owing to the significantly larger critical transverse channeling energy.[42]

In Fig. 9 we show the dependence of the efficiency of deflecting $^{12}_{6}$C nuclei of energy 6 GeV/nucleon by (a) silicon and (b) tungsten crystals, bent at an angle of 100 mrad along the (110) planes, on the bend radius. The points are the results of a computer simulation.[42] The deflection efficiency of the tungsten crystal is more than an order of magnitude higher than that of the silicon crystal. However, for small deflection angles the tungsten crystal cannot give a significant gain in the efficiency.

When bent crystals are used to extract the particles of a beam halo from a collider, the extraction efficiency is largely determined by multiple passages of the circulating particles through the crystal.[11,43,44] The contribution of multiple passages depends strongly on the multiple-scattering angle and on the losses in inelastic nuclear interactions in the crystal, which are larger for tungsten. The optimal crystal and its parameters for beam extraction from an accelerator must be chosen specifically for each particular situation.

3.6. The channeling of relativistic nuclei

The possibility of using bent crystals for steering beams of relativistic nuclei has been successfully demonstrated at Dubna[14] and CERN.[45] As the particle charge increases in going from protons to nuclei, the force acting on a particle in the channel increases, and the depth of the planar-channel potential well of the crystal becomes $U(x)=Z_1U^1(x)$, where $U^1(x)$ is the planar potential for protons. The critical transverse energy of the particles E_{xc} increases accordingly. However, channeling parameters determined by the averaged potential, such as the spatial period of oscillation of the particles in a planar channel λ and the critical channeling angle ϑ_c, remain invariant with respect to $p_z=p/Z_1$, where p is the total particle momentum.[46]

The critical bend radius of a crystal is also invariant with respect to p_z:

$$R_c(p_z)=\frac{p_z c}{e\mathscr{E}_{\max}}, \tag{63}$$

and so in a bent crystal at a given bend radius R the channeling parameters are invariant. This implies identical probability for particle capture into the channeling regime, which for a beam with Gaussian angular distribution has the form [see (16a)]

$$P_c(p_z;R,\xi)=\frac{1}{d_p}\int_{r_c}^{x_{\rm ch}} Erf\left[\frac{1}{\sqrt{2}\xi}\left(1-\frac{U^1_{\rm eff}(x_0,R)}{E^1_{xc}(R)}\right)\right]dx_0, \tag{64}$$

where $\xi=\bar{\vartheta}_x/\vartheta_c$, x_0 is the coordinate of the point where the particle enters the channel, $x_{\rm ch}$ is the coordinate determining the channeling region in a bent channel, and $U_{\rm eff}(x_{\rm ch})=E_{xc}$.

The dechanneling length of particles in a crystal is mainly determined by scattering on the crystal electrons, and its dependence on the particle parameters is not expressed only in terms of p_z—there is an additional logarithmic dependence on Z_1. It follows from (50) and (51) that a good estimate of the dechanneling length is

$$S_{1/e}(p_z,Z_1;R)=\frac{2}{\mu^2_{0,1}}\frac{E^1_{xc}}{NZ_e\pi e^4}\frac{p_z c(1-R_c/R)^2}{\ln(Z_1 r_a\sqrt{2p_z cE^1_{xc}/\hbar c})}. \tag{65}$$

However, the Z_1 dependence is weak, and, as shown by experiment,[14] the dechanneling lengths for protons and oxygen nuclei with $p_z=9$ GeV/c in a bent silicon crystal coincide within the experimental error.

Therefore, the beam deflection efficiency of a bent crystal must also be invariant with respect to p_z. In fact, a recent CERN experiment[45] on the deflection of ultrarelativistic lead nuclei of momentum 33 TeV/c by a bent silicon crystal showed that the fraction deflected by the crystal is approximately the same as for protons with the same p_z. The deflection efficiencies obtained in a computer simulation coincided with the experimental values to within 15%.

In a straight crystal the observed dechanneling lengths for protons are largely determined by processes of recapture into the channeling regime, whereas for heavy nuclei the strong growth of the cross section for inelastic interactions decreases the recapture probability. As a result, the invariance of the dechanneling lengths with p_z in a direct crystal is violated.[47]

4. THE MODELING OF PARTICLE TRAJECTORIES IN A CRYSTAL

The most flexible and detailed method of studying channeling in crystals is modeling of the particle trajectories in a crystal. Moreover, study of the particle trajectories allows the study of more complicated processes such as particle extraction from an accelerator using a bent crystal. The model of binary collisions used in the first computer experiment,[3] where the particle trajectory is formed as a result of interaction with each atom of the crystal along the particle path, does not allow study of crystals of size on the scale of centimeters, owing to the large amount of computer time required.

Methods of grouping collisions, one of which is the segment model,[48] are usually used to model the passage of charged particles through matter. In the segment model the particle path is divided into segments of definite length. The change of state of the particle at the end of the segment is determined by multiple scattering. The transition probability density in phase space

$$(\mathbf{r}=0,\boldsymbol{\Omega}=\boldsymbol{\Omega}_0,E=E_0)\rightarrow(\mathbf{r},\boldsymbol{\Omega},E)$$

is written as the product of four factors:

$$P(\mathbf{r},\boldsymbol{\Omega},E)=P(E|l)P(\boldsymbol{\Omega}|l)P(z|\boldsymbol{\vartheta},l)P(\boldsymbol{\rho}|\boldsymbol{\vartheta},l),$$

respectively describing the energy distribution, the distribution in the direction $\boldsymbol{\Omega}$, the distribution of longitudinal displacements z, and the distribution of transverse displacements $\boldsymbol{\rho}$ of particles on a segment l.

The length of a segment is usually chosen such that energy losses can be neglected. For heavy particles it is also possible to neglect the longitudinal displacements because they are relatively small: in particle channeling in a crystal they are significantly smaller than the particle oscillation length in the channel, $z\ll\lambda$. The angular distribution of charged particles in multiple scattering is described by the Molière theory.[49] The Molière distribution can be represented as a series whose first term is a Gaussian. The distribution of transverse displacements is also a normal distribution.[48] The transverse displacement and the scattering angle of a particle are correlated in multiple scattering. The displacement and angle of the combined distribution in the one-dimensional case are modeled as[50]

$$\Delta x=\eta_1 l\bar{\theta}/\sqrt{12}+\eta_2 l\bar{\theta}/2,\quad \Delta\vartheta_x=\eta_2\bar{\theta}, \tag{66}$$

where η_1 and η_2 are random numbers from a Gaussian distribution with zero average and unit dispersion, and $\bar{\theta}$ is the rms multiple-scattering angle of the particles in the layer in question.

In an oriented crystal the multiple scattering of charged particles on atoms is separated into a coherent part, in which the average change of direction of the particle momentum is described by the continuous potential of planes or chains of atoms, and an incoherent part, arising from scattering on electrons and the real discrete structure of the crystal, including thermal displacements of the atoms from lattice sites. When speaking of particle multiple scattering in channeling in a crystal, it is scattering on electrons and the scattering due to the difference between the real crystal potential and the continuous potential that we have in mind; they both tend to change the particle transverse energy.[1] They differ significantly from ordinary multiple scattering in amorphous matter, which is mainly due to Coulomb scattering on nuclei.

In Ref. 51 the passage of particles through a crystal with planar orientation was calculated using a fast computer model based on the continuous approximation for the potential of a set of bent atomic planes of the crystal with step-by-step inclusion of multiple scattering on the electrons and nuclei of the crystal.

4.1. Modeling the set of atomic planes

When a particle enters a crystal at a small angle to the bent atomic planes, its trajectory in the crystal can, in a first approximation, be calculated by numerically solving the equation of motion in the effective potential (18) of the system of bent atomic planes:

$$\ddot{x}(t)=-\frac{c^2}{E}\frac{d}{dx}U_{\text{eff}}(x,R). \tag{67}$$

When calculating the passage of particles through the crystal the change of the particle longitudinal velocity can be neglected, since it is relatively small. Then each step of the time integration of the equations of motion corresponds to the particle traveling a distance $\Delta z=v\Delta t$ in the crystal. In the continuous approximation the particle transverse energy in the crystal $E_x=m\gamma\dot{x}^2/2+U(x)$ is an integral of the motion, and so the integration step Δt is chosen from the condition that E_x be conserved. The continuous potential of the set of atomic planes was calculated using the Molière approximation for the atomic potential (5) and was averaged over thermal oscillations of the atoms.

After the particles travel a distance $\Delta z_s=v\Delta t_s$ in the crystal, where $\Delta t_s\geqslant\Delta t$, the change of the particle transverse velocity due to multiple scattering on the crystal electrons and nuclei is calculated. The step size Δz_s is bounded below by the requirement that the theory of multiple scattering be valid. The usual upper bound on Δz_s, from the condition that the particle energy loss be negligible, is always satisfied for heavy, high-energy particles in channeling experiments. However, in a crystal, where the particle motion is governed by a continuous potential, the change of the transverse velocity acquired by a particle owing to multiple scattering in a layer Δz_s will induce a change of a different magnitude in the transverse energy depending on the location of the scattering point in the channel cross section. Therefore, the step size Δz_s must be bounded above: $\Delta z_s\ll\lambda$.

The mean-square particle deflection angle per unit pathlength in the multiple scattering of particles on nuclei was calculated in the Ohtsuki–Kitagawa approximation:[52]

$$\frac{\overline{\Delta\vartheta^2}}{\Delta z}_n(x)=\frac{\overline{\Delta\vartheta^2}}{\Delta z_R}P_n(x), \tag{68}$$

$$\frac{\overline{\Delta\vartheta^2}}{\delta z_R}=\frac{1}{L_r}\left(\frac{E_s}{pv}\right)^2,\quad P_n(x)=\frac{d_p}{(2\pi u_1^2)^{1/2}}\exp(-x^2/2u_1^2),$$

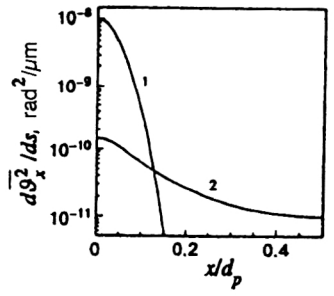

FIG. 10. Dependence of the mean squared deflection angle of 1-GeV protons per unit path length owing to multiple scattering on (1) nuclei and (2) electrons in a silicon crystal as a function of the distance of the particle to the wall of the (110) channel.

where $\overline{\Delta\vartheta^2}/\Delta z_R$ is the corresponding value for an amorphous medium, $P_n(x)$ is the transverse distribution of the atoms of a plane due to thermal motion, $E_s=21$ MeV, and L_r is the radiation length. The inclusion of nonlocality of the interaction leads to slower falloff of the multiple scattering on nuclei at large distances from the planes.[53] However, this can be neglected, because scattering on electrons dominates in the central part of the channel.

In collisions with atomic electrons, a significant transverse momentum is transferred to a heavy relativistic particle in near collisions. Using the proportionality to the energy loss, for the average squared deflection angle per unit pathlength we find[1]

$$\frac{\overline{\Delta\vartheta^2}}{\Delta z_e}(x)=\frac{m_e}{2m\gamma E^*}\left(-\frac{dE}{dz}\right)\frac{\rho(x)}{NZ_2}, \tag{69}$$

$$-\frac{dE}{dz}=\frac{4\pi Z_1^2e^4}{m_ev^2}NZ_2\left[\ln\left(\frac{2m_e\gamma^2c^2\beta^2}{I}\right)-\beta^2\right],$$

where $-(dE/dz)$ is the specific ionization energy loss, I is the average ionization potential (for silicon we used the value $I=165$ eV), and $\rho(x)$ is the electron density in a planar channel of the crystal, determined in terms of the planar potential from the Poisson equation, using the Molière approximation and calculated with inclusion of the contribution of the two neighboring planes.

The trajectories of particles with large transverse energies, $E_x>E_{xr}$, were calculated as in amorphous matter; for protons in silicon we took $E_{xr}=400$ eV. Here the tracking step was increased, but constrained by the condition that the particle eventually enter the region in which $E_x<E_{xr}$.

In Fig. 10 we show the mean-square particle deflection angle per unit path length in multiple scattering on nuclei and electrons as a function of the distance to the channel wall for 1-GeV protons. We see that at a distance greater than $2u_1$ from the channel walls, the main contribution to the change of the particle transverse energy comes from scattering on the crystal electrons.

In calculating the multiple-scattering angle in (69) we took into account all near collisions with electrons with energy transfer up to the maximum allowed value $T_{\max}$, although the upper limit of the multiple-scattering region corresponding to energy transfer $T_c=T(\vartheta_c)$ lies below $T_{\max}$ (Ref. 54). The higher value of the upper limit in the ionization logarithm is compensated by simultaneously raising the lower limit, taken to be the average ionization potential I, although the main contribution to dechanneling comes from scattering on outer-shell electrons, the ionization potential of which is smaller than the average value. The results of computer experiments using this model agree satisfactorily with the available experimental data. A more correct treatment would be to include the contribution to scattering from individual shells of the crystal atoms.

In addition to the change of angle due to multiple scattering, at each step we simulated an inelastic nuclear interaction of the particles in the crystal, as a result of which the primary particle (a proton or nucleus) disappears, and the process of modeling its passage through the crystal is terminated. The nuclear interaction probability in a layer Δz_s for a particle was defined as

$$P_{\text{in}}=1-\exp(-\Delta z_s/L_{\text{in}})\simeq\Delta z_s/L_{\text{in}}, \quad L_{\text{in}}=L_n/\langle P_n\rangle, \tag{70}$$

where L_{in} is the mean free path between inelastic nuclear interactions, calculated with allowance for the average density of nuclei along the particle trajectory in a given layer $N\langle P_n\rangle$; $L_n=45.5$ cm is the mean free path before interacting in amorphous silicon.

4.2. The modeling of dechanneling

The dechanneling of protons and pions of energy from 60 to 200 GeV in a bent silicon crystal has been studied experimentally at Fermilab.[24] This experiment used particle selection according to the ionization energy losses in the leading straight part of the crystal, measured by an intrinsic surface-barrier detector. The uniform bending of the crystal, obtained by means of a thin layer of ZnO deposited from the outside of the crystal, eliminated centrifugal dechanneling of particles. Particle dechanneling occurred only owing to multiple scattering in the crystal. The uniformity of the crystal bending made it possible to establish a simple correspondence between the particle deflection angle ϑ_x and the distance S along the crystal which a particle traveled before leaving a bent planar channel: $S=\vartheta_xR$. Thus, the dependence of the channeled fraction on the beam penetration depth in the crystal was studied in detail in the experiment. It was well fitted by an exponential function.

The dependence of the dechanneling length on the particle energy obtained experimentally for a silicon crystal bent along the (110) planes, at room temperature and cooled to -145 °C, is shown in Fig. 11a. The experimental results confirm the absence of proportionality of the dechanneling length to the particle energy in a bent crystal, as was first shown in Ref. 28. In addition, the experiment revealed a significant enhancement of the temperature dependence of the dechanneling length with increasing particle energy.

In Fig. 11a we also show the results of a computer simulation. The particle angular distribution at the entrance to the crystal was assumed to be uniform, and particles were also selected according to the ionization energy losses. The results of the modeling are in good agreement with the dechanneling lengths and their variation with particle energy, and

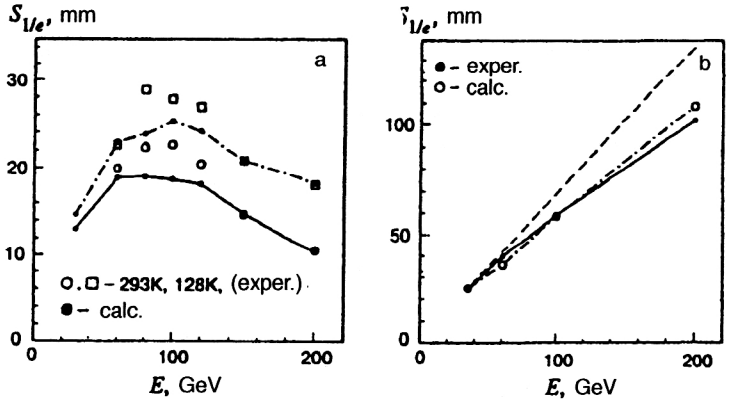

FIG. 11. Dependence of the dechanneling length on the particle energy: (a) for a silicon crystal bent along the (110) planes at room temperature and cooled to −145°; (b) for a straight crystal.

they reflect the enhancement of the temperature dependence at higher particle energies. The latter is due to the fact that the effective bending of the crystal $\rho = R_c(E)/R$ increases, and so when the trajectories of channeled particles are very close to the channel wall there is a large contribution to dechanneling from scattering on nuclei.

In Fig. 11b we show the experimental[36] and calculated E dependences of the dechanneling length in a straight crystal. The agreement with experiment is good. The difference between the observed dependence and the linear one (dashed line) due to the logarithmic factor in the electron coefficient of friction is about ten percent in the energy range studied.

5. QUASICHANNELING IN A BENT CRYSTAL

The behavior of quasichanneled or above-barrier particles with transverse energies above the critical channeling energy E_{xc} but moving through a crystal at small angles to the atomic planes, $\vartheta_x \ll 1$, is also largely determined by the continuous potential and has special features in a bent crystal.

For quasichanneled particles, experimental studies have discovered capture by bent planar channels in the crystal volume (volume capture),[55,56] while a computer experiment has revealed deflection by a bent crystal in the direction opposite to the bend (volume reflection).[31] The processes of volume reflection and capture are shown schematically in Fig. 12.

A kinetic equation for quasichanneled particles in a bent crystal was proposed in Refs. 46 and 57. It can be used together with the equation for the channeled fraction to study processes of exchange between the fractions. Processes originating in the quasichanneled fraction of the beam have been studied in Refs. 25, 31, 33, and 51 by computer simulation.

5.1. Volume reflection

Calculation of the passage of quasichanneled particles through a bent crystal in the approximation of a continuous planar potential using (32) revealed[31] that for bend radius $R \gg R_c$ the particles are deflected to the side opposite the bend by an angle of about $2\vartheta_c$, and that the spread of deflection angles is small. The observed deflection can be viewed as particle reflection by the bent atomic planes originating in the crystal volume, i.e., volume reflection. Volume reflection also occurs for negatively charged particles, but their reflection angle is smaller.

The deflection of particles by a bent crystal in the continuous-potential approximation is an idealized situation. The difference between a real, three-dimensional crystal potential and the continuous one, and also particle scattering on electrons, lead to a spread in the transverse momentum of the reflected particles. The ratio of the particle reflection angle for the continuous potential and the angular spread introduced by multiple scattering determines whether or not volume reflection is experimentally observable, and depends on the particle energy.

The size S_{vr} of the crystal region in which volume reflection occurs is determined by the critical channeling angle and the bend radius of the crystal, $S_{vr} \sim R\vartheta_c$. Since particle scattering in the average field of the planes of a bent crystal is identical for a given relative bending of the crystal

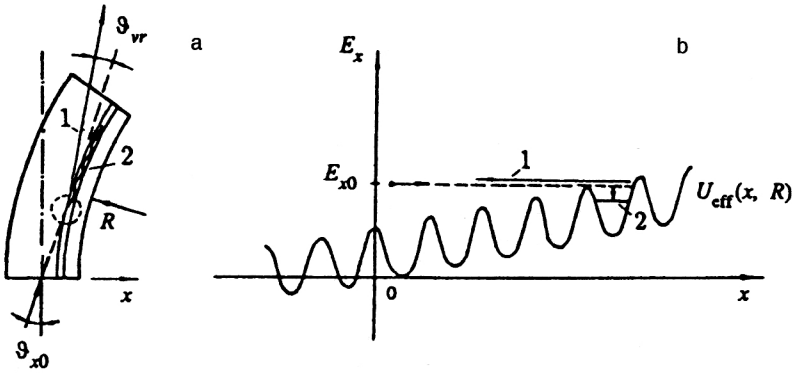

FIG. 12. (a) Schematic depiction of (1) volume reflection and (2) volume capture into the planar-channeling regime in the region tangent to the planes (shown by the dashed line) for a particle entering a bent crystal at an angle $\vartheta_{x0} > \vartheta_c$; (b) the same in (x, E_x) space near the turning point in the effective potential $U_{eff}(x, R)$.

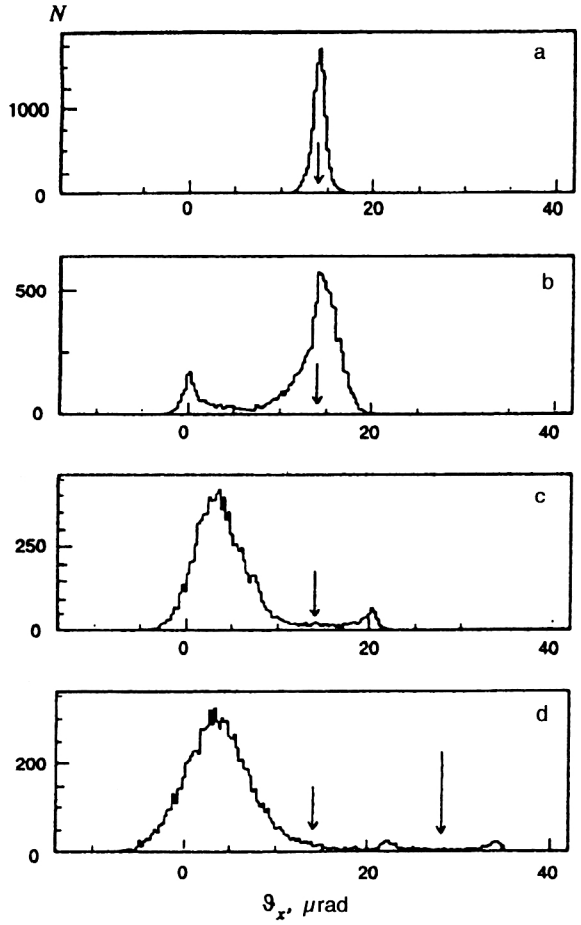

FIG. 13. Illustration of the volume reflection of particles by a bent crystal. Angular distributions of 900-GeV protons at various depths in a silicon crystal bent along the (110) planes. The small arrow is the initial direction of the beam, and the long arrow in (d) is the bending angle at the given depth.

$r=R/R_c$, if the deflection angle is expressed in terms of the critical channeling angle,[31] then at fixed r the size of the region of volume reflection increases with the particle energy, $S_{vr}\sim rR_c\vartheta_c\sim E^{1/2}$.

The broadening of the beam in volume reflection in a bent crystal over a length S_{vr} due to multiple scattering can be estimated by assuming that for super-barrier particles the scattering is the same as in an amorphous target:

$$\overline{\Delta\vartheta^2}_{vr}=S_{vr}\cdot\frac{\overline{\Delta\vartheta^2}}{\Delta z_R}\sim E^{-3/2},\quad \frac{\langle\overline{\Delta\vartheta^2}_{vr}\rangle^{1/2}}{\vartheta_c}\sim E^{-1/4}.$$

The relative angular spread of the particles reflected in the crystal volume decreases as $E^{-1/4}$ with increasing particle energy, and at some energy becomes smaller than the reflection angle.

Therefore, at high particle energies volume reflection in a bent crystal is not suppressed by multiple scattering and is clearly manifested in the angular distributions for a parallel beam. In Fig. 13 we show the angular distributions calculated in Ref. 25 for 900-GeV protons at various depths in a silicon crystal bent along the (110) planes with radius $R\simeq 100R_c$, which amounts to 150 m, for an incident-beam slope angle $\vartheta_0\simeq 2\vartheta_c$.

In Fig. 13a the particles have not yet reached the reflection region. The center of the angular distribution coincides with the initial direction (small arrow), and the width is determined by particle multiple scattering in the crystal. In Fig. 13b part of the beam has already undergone volume reflection, and a maximum has appeared in the angular distribution at a distance of about $2\vartheta_c$ on the side opposite the bend. Figure 13c is for the depth corresponding to the geometrical point where the incident particles are tangent to the bent planes, $S=2\vartheta_cR$. This is half of the reflection region; at this depth a large part of the beam already forms a clearly expressed maximum of reflected particles, and the width of this maximum is smaller than the displacement relative to the initial direction. Figure 13d shows the angular distributions at the exit from the reflection region of length $S=4\vartheta_cR$. The long arrow indicates the bending angle $\alpha=4\vartheta_c$. The clearly expressed symmetric maxima about the bending angle at a distance of about ϑ_c are formed by particles which were captured into the channeling regime in the crystal volume (see below) and deflected by the crystal, following the bent channels.

Volume reflection can be clearly seen experimentally for high-energy particles by using a short crystal of length $\sim R\vartheta_c$ and a narrow beam of angular spread $\sim\vartheta_c$, which can be formed by means of an additional shaper crystal. The volume reflection of particles in a bent crystal comes into play when the crystal is used as a deflector for extracting beams of high-energy particles from accelerators. For example, in Ref. 58 it was shown by modeling that volume reflection leads to asymmetry of the orientational dependence of the efficiency of beam extraction from cyclic accelerators by means of a crystal.

5.2. Volume capture of particles

When a beam of particles intercepts a bent crystal, a large part of the beam is reflected in the region tangent to the bent planes. However, there are particles which are captured by bent planar channels and which can be deflected by the crystal by an angle equal to the bend angle.

Volume capture in a bent crystal was discovered experimentally[55] by using a beam of 1-GeV protons. Three surface-barrier detectors were created in a silicon crystal bent along the (111) planes, which allowed separation of the channeled particles at various stages of the beam passage through the crystal by means of the ionization energy losses. The ionization-loss spectra obtained in the experiment showed that enrichment of particles with small energy losses occurs, which is convincing evidence for the capture of particles from the quasichanneled fraction into the channeling regime inside the crystal volume.

Attempts have been made to find specific mechanisms which dissipate the particle transverse energy in a bent crystal.[59] However, the mechanism for the volume capture of particles in a uniformly bent crystal, like that in a straight crystal,[60] is multiple scattering, which can induce transitions of particles not only from the channeled fraction to the unchanneled one, but vice versa. In Ref. 51 it was shown that

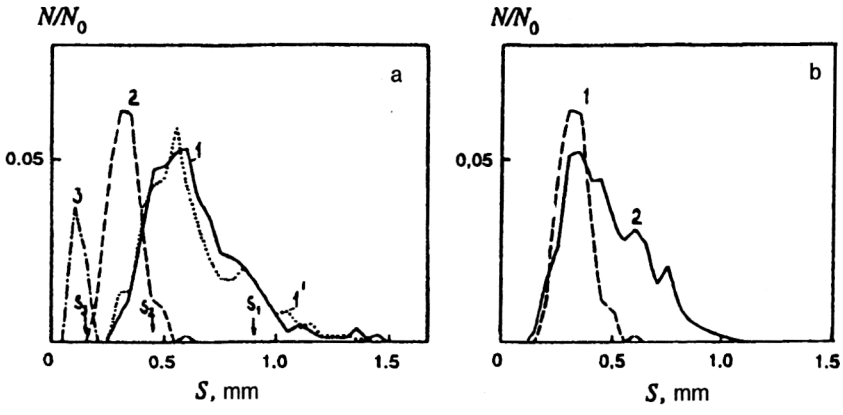

FIG. 14. Fraction of particles captured for the first time by bent (110) channels of silicon in a layer of thickness 50 μm as a function of the beam penetration depth (a) for 200-GeV protons at various crystal bend radii R in meters: (1) 30, (2) 15, and (3) 5. Curve 1′ is for $T=-145$ °C; (b) for (1) 200-GeV and (2) 100-GeV protons at $R=15$ m.

this capture mechanism is sufficient for explaining the experimental results.[55]

The necessary condition for the volume capture of particles into the channeling regime is high density of particles with transverse energies close to the critical value E_{xc}. In a straight crystal this density is very small at orientation angles of the incident beam significantly larger than the critical angle, because it is determined only by the diffusion of particles from the initial state as a result of multiple scattering, and so volume-capture events are rare.

The bending of a crystal significantly increases the range of orientation angles for which volume capture of particles in the crystal is possible. This range is determined by the bending angle, and not by the critical channeling angle. The direction of the particle momentum at the entrance to the crystal determines the presence of a capture region, where it becomes close to the direction of tangents to the planes. Particles moving in a bent crystal approach or recede from the capture region. This can be viewed as a manifestation of an additional mechanism of particle drift to the capture region in a bent crystal.

Owing to the bending of the crystal, the capture region is localized, and the fraction of particles dechanneled and recaptured is relatively small.[33] This is in contrast to the case of a straight crystal, where repeated capture of particles into the channeling regime is significant, because the particles spend a long time in the near-barrier region of transverse energies and leave it only owing to multiple scattering.

In a computer simulation[33] it was shown that volume capture decreases with decreasing bend radius and increasing particle energy, and is weakly dependent on the crystal temperature. In Fig. 14 we show the depth dependence of the volume capture of protons by bent (110) channels of silicon for various bend radii and temperatures of the crystal (a) and for various particle energies (b). The capture maximum is shifted to the entrance face of the crystal as the bend radius R decreases, and lies closer to it than the tangency point $S_i=\vartheta_0 R_i$, owing to intense multiple scattering. This difference increases with increasing bend radius. The total number of captured particles, given by the area under the curve, decreases with decreasing R. A change of the crystal temperature has very little effect on the volume capture, owing to the small change of the characteristic angles ϑ_c and ϑ_{ms}; see curves 1 and 1′ in Fig. 14a. Decrease of the particle energy for fixed bend radius, which increases the multiple scattering $\vartheta_{ms}\sim 1/E$ and the extent of the capture region $S_{vc}\sim R\vartheta_c \sim E^{-1/2}$, where the direction of the particle momentum is nearly tangent to the bent planes, tends to increase the volume capture (Fig. 14b).

Experimental studies of volume capture in bent crystals were later performed at IHEP, using a 70-GeV proton beam.[61,62] It was shown that the probability for volume capture grows in proportion to the bend radius of the crystal.

The probability for volume capture of particles depends on the capture depth $\Delta E_{vc}=U_m-E_{xc}(r_c)$, where U_m is the height of the potential barrier dividing adjacent planar channels in a bent crystal, i.e., it depends on the choice of the distance of critical approach to the channel walls r_c (Ref. 63). In a computer experiment[25] the capture probability was defined as the ratio of the number of captured particles summed over the entire length of the crystal and the total number of particles in the incident beam. For a proton energy of 1 GeV and using $r_c=a$, which corresponds to the critical transverse energy $E_{xc}\simeq 14$ eV, the capture probability was about 11%, which is close to the value found in the experiment of Ref. 55.

In Ref. 62 a simple expression was proposed for estimating the probability for the volume capture of particles in a bent crystal. The authors started from the reversibility principle,[1] according to which the probability for a particle transition from the unchanneled fraction to the channeled fraction is equal to the probability for particle dechanneling over a length dz. Assuming that the dechanneling is exponential, the probability is $P_{\text{dec}}=|df_{\text{ch}}|/f_{\text{ch}}=dz/S_d$, where S_d is the dechanneling length. Then over the length $R\vartheta_c$ characterizing the extent of the capture region, the probability of volume capture is given by

$$P_{vc}\simeq\frac{R\vartheta_c}{S_d}. \tag{71}$$

This definition of the capture probability can be valid for crystal bend radii which are not too large and for particle capture into deep levels in the channel potential, for which $R\vartheta_c\ll S_d$. For bending far from critical, when the critical angle and the dechanneling length in a bent crystal have the

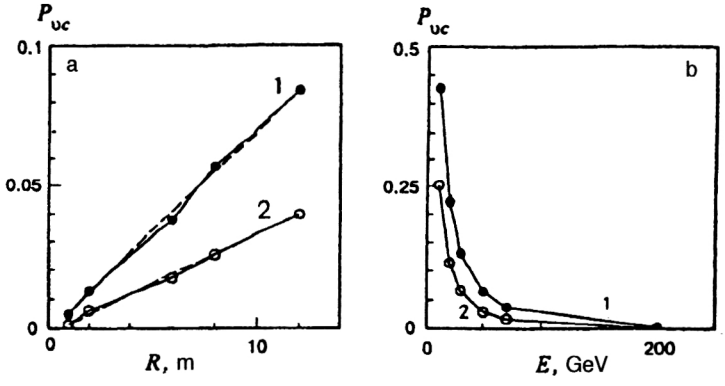

FIG. 15. Dependence of the probability for volume capture by bent (110) channels of silicon on (a) the crystal bend radius for 70-GeV protons and (b) the proton energy, for $R=6$ m, at various distances of critical approach of the particles to the planes: (1) $r_c=2u_1$ and (2) a.

same energy dependence as in a straight crystal and are practically independent of R, it follows from (71) that $P_{vc} \sim RE^{-3/2}$ (Ref. 62).

In Fig. 15 we show the dependence, obtained in a numerical experiment,[25] of the probability for volume capture on (a) the crystal bend radius and (b) the particle energy for two values of r_c. The probability for particle capture into deep levels of the channel potential well actually grows linearly with increasing bend radius. A fit to the capture dependence on the particle energy shows that $P_{vc} \sim E^{-3/2}$ for fixed bend radius of the crystal, which also confirms the validity of (71) for estimating volume capture.

5.3. Gradient volume capture

In a bent crystal, along with the appearance of a new centrifugal mechanism for particle dechanneling on a segment with growing curvature, the reverse process of "centrifugal" or "gradient" volume capture[9] of particles into the channeling regime becomes possible for decreasing curvature. Gradient capture is due to the increased depth of the effective potential well of the planar channels along the crystal.

Gradient volume capture was discovered in a computer experiment[64] which was the reverse of the experiment in which centrifugal dechanneling was first studied.[38] Calculations carried out in the continuous-potential approximation showed that a certain fraction of particles is captured into the channeling regime in going from a uniformly bent to a straight part of the crystal.

The probability for gradient volume capture in a bent crystal with slowly decreasing curvature of the planar channels was determined in Ref. 65. The change of the particle transverse energy E_x as a result of decrease of the curvature Δk over a length Δz is determined by the average transverse coordinate of the particle $\langle x \rangle$ over this length $\Delta E_x = \Delta k \langle x \rangle$. The corresponding change of the critical transverse energy $E_{xc}=U_{\text{eff}}(-x_c)$ is $\Delta E_{xc}=-\Delta k x_c$. Therefore, the change of the particle energy E_x relative to the change of height of the potential barrier over a length λ in the approximation $k'=\text{const}$ is

$$\delta E_x=\Delta E_x-\Delta E_{xc}=k'(\langle x \rangle+x_c)\lambda. \tag{72}$$

The average particle coordinate over an oscillation period is determined by the location of the shifted orbit of the channeled particles $\langle x \rangle = x_0$, and on a segment with decreasing curvature $\delta E_x<0$. This implies that quasichanneled particles with E_x in the range $(E_{xc}, E_{xc}+\delta E_x)$ can be captured into the channeling regime.

The total spread of the transverse energies of quasichanneled particles near the turning point in the effective planar potential of a bent crystal is determined by the increase over the channel width $\Delta U = d_p(pv/R)$. Assuming that the particle distribution over the interval ΔU is uniform, for the probability of gradient capture we have[65]

$$P_{bc}=-\frac{\delta E_x}{\Delta U}=\frac{R'\lambda}{R}\frac{x_c}{d_p}\left(1+\frac{\langle x \rangle}{x_c}\right), \tag{73}$$

where $R'=dR/dz$. In the approximation of a parabolic potential,

$$P_{bc}=\frac{R'\lambda}{R}\frac{x_c}{d_p}\left(1-\frac{R_c}{R}\right). \tag{73a}$$

When the bending of the crystal is much smaller than the critical value, $R \gg R_c$,

$$P_{bc}\simeq\frac{R'\lambda}{2R}\sim\lambda/L_b, \tag{73b}$$

where L_b is the length of the segment with uniformly decreasing curvature. The probability of centrifugal particle capture grows with energy as $E^{1/2}$, while capture due to multiple scattering decreases.

The total probability for particle capture into the channeling regime due to the gradient mechanism in a crystal with radius uniformly increasing in the interval (R_c, R) for a broad beam coincides with the probability for face capture into a channel of radius R (Ref. 65), i.e., the creation of a region with decreasing curvature at the entrance to the crystal does not increase the efficiency of a crystal deflector.

6. IONIZATION ENERGY LOSSES

It is well known that the ionization energy losses of fast charged particles in channeling in a crystal differ from the losses in the misoriented case, when the direction of the particle momentum is far from densely packed directions and planes. The losses in near collisions are proportional to the local electron density $\rho(x)$, which for channeled particles differs from the average over the crystal NZ_2 and is determined by the particle trajectory. Since near and distant collisions of particles with the matter electrons give roughly

identical contributions to the losses at high energies, then, assuming that the contribution of distant collisions is independent of the particle trajectory, for the stopping power μ, according to Lindhard,[1] we have

$$\mu(x)=\mu_a[(1-\alpha)+\alpha\rho(x)/(NZ_2)], \tag{74}$$

where $\alpha\simeq 1/2$ is the separation constant. In a misoriented crystal the electron density averaged along the particle trajectory is equal to the average NZ_2, and the stopping power is the same as in amorphous matter, μ_a. In channeling, positively charged particles move through a region of the crystal with lower electron density, and their stopping power is usually smaller than μ_a. According to (74), the minimum losses for well channeled particles moving in the center of the channel can be almost half the loss in the misoriented case, $\mu(0)\simeq 0.5\mu_a$.

Measurement of the particle ionization losses by intrinsic surface-barrier detectors gives information on the particle state during passage through the crystal.[55,66] Such a detector at the crystal entrance is used to orient the crystal relative to the beam. When the beam is oriented along a plane or axis of the crystal, the loss spectrum recorded by the intrinsic detector contains an additional maximum with losses smaller than μ_a due to channeled particles. The authors of Ref. 67 managed to increase the channeled fraction of a beam incident on a crystal by means of the loss spectra recorded by an intrinsic detector. They varied the beam dimensions in the transverse plane, using magnetic elements of the channel, thereby decreasing its spread. This method can be used to obtain beams with spread much smaller than that for other methods. A beam of 450-GeV protons shaped in this manner had a spread of less than 3 μrad, which made it possible to obtain a record-setting deflection efficiency of a bent crystal: 50% for small deflection angles.

The use of bent crystals to isolate the deflected fraction of a beam offers the additional possibility of studying the ionization energy losses of well channeled particles possessing small transverse energies upon entering the crystal, and completely eliminating the contribution to the loss spectra from unchanneled particles, as was shown in the experiment of Ref. 67. The selection of particles with given entrance and exit angles used earlier did not allow this to be achieved.[66]

The authors of Ref. 68 proposed a kinetic equation for the channeled and quasichanneled fractions of the beam separately, in order to study theoretically the ionization losses of particles in a bent crystal, taking into account the evolution of their transverse-energy distribution due to multiple scattering. The ionization-loss spectra of protons passing through silicon crystals bent along the (111) planes were studied in Ref. 69 by modeling. The modeling method, which uses the stopping power and electron density calculated along the particle trajectories, does not require large statistics and leads to good agreement with experiment for the most probable energy losses and their spread, both for the entire beam and for the deflected fraction.

The particle trajectories in the crystal were calculated[69] by modeling the set of atomic planes. The average energy loss of a particle in each layer

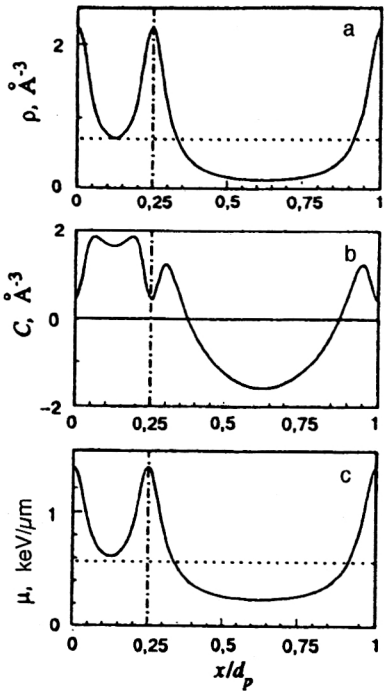

FIG. 16. Change of (a) the average electron density, (b) the correction C, and (c) the stopping power in the cross section of the (111) channel of silicon. The dashed lines are for the misoriented case, and the dot–dash line divides the regions of narrow and wide (111) channels.

$$\bar{\Delta}_{\rm tr}=\frac{dE}{ds}(\rho_{\rm tr},C_{\rm tr})S_L \tag{75}$$

was calculated by using the stopping power from Ref. 70, which depends on the particle trajectory in the crystal:

$$\mu(x)\equiv-\frac{dE}{ds}(x)=\frac{2\pi Z_1^2e^4}{mv^2}\left\{[NZ_2+\rho(x)]\times\left[\ln\frac{2mv^2\gamma^2}{I}-\beta^2\right]+C(x)-NZ_2\delta\right\}, \tag{76}$$

$$C(x)=\sum_{K_x\neq 0}\rho(K_x)e^{iK_xx}\ln(2mI/\hbar^2K_x^2), \tag{77}$$

where $C(x)$ is a correction taking into account the nonuniformity of the electron distribution in the channel, $\rho(K_x)$ is the Fourier coefficient of the expansion of the electron density $\rho(x)$ averaged along the crystal planes, K_x is the reciprocal lattice vector of the crystal, δ is the correction for the density effect, and $\rho_{\rm tr}$ and $C_{\rm tr}$ are the values of the electron density and the correction C averaged along the particle trajectory in the layer.

In Fig. 16 we show the variation of (a) the average electron density, (b) the correction C, and (c) the stopping power in a cross section of the (111) channel of silicon, calculated at room temperature in the Molière approximation. The behavior of both the electron density and the correction results from the decrease of the stopping power for particles moving in a wide channel, and, conversely, its increase when the particles move in a narrow channel, in relation to the misoriented case.

The average energy loss $\bar{\Delta}^j_{\rm tr}$ and the average electron density $\rho^j_{\rm tr}$ calculated along the trajectory of the jth particle in a crystal layer determine the energy-loss distribution, which, according to Landau, has the form

$$f^j(\Delta_i)=\frac{1}{\xi^j}\varphi(\lambda^j_i), \quad \int_0^\infty f(\Delta)d\Delta=1, \tag{78}$$

$$\lambda^j_i=\frac{\Delta_i-\bar{\Delta}^j_{\rm tr}}{\xi^j}-\beta^2-0.423-\ln(\xi^j/T_{\max}),$$

$$\xi^j=\frac{2\pi e^4}{mv^2}\rho^j_{\rm tr}S_L,$$

where $\varphi(\lambda)$ is the universal Landau function and λ is its parameter. The thickness of a crystal layer in the modeling was $S_L=2.5$ mm, which ensured that the condition for the Landau distribution to be applicable, $T_k \ll \xi \ll T_{\max}$, was satisfied, where T_k is the electron binding energy and $T_{\max}$ is the maximum energy transferred to an electron. The total ionization energy-loss distribution in the layer was obtained by summing the contributions from all the particles of the beam.

In the experiment of Ref. 67, a silicon crystal of length 50 mm was bent along the (111) planes, using a three-point bender, which produces nonuniform bending with maximum curvature near the central support. In the modeling, the crystal dimensions and shape were taken to be the same as in the experiment.

In Fig. 17a we show the ionization energy-loss spectrum of protons in the first layer of the crystal oriented along the (111) planes, obtained by modeling. The spectrum contains two maxima, at $\Delta^1_{mp}\simeq 0.6\Delta^R_{mp}$ and $\Delta^2_{mp}\simeq 1.18\Delta^R_{mp}$, where Δ^R_{mp} are the most probable losses in the misoriented case. The first peak is formed by particles channeled in wide channels with fairly low transverse energies. The second is due to particles channeled in narrow channels plus particles channeled in wide channels, but possessing large transverse energies, and also by quasichanneled, near-barrier particles. For all these beam fractions the average electron density is higher than in the misoriented case, which is a consequence of not only the increased loss probabilities, but also the spread, which causes the width of the maximum of high losses to be 54% larger than the width for the misoriented case. The calculated spectrum is compared with the experimental one,[67] and there is seen to be good agreement in the width and the relative location of the maxima.

In Fig. 17b we show the spectrum of the entire beam in the first layer, and also the spectrum of ionization energy losses separately for the deflected fraction of the beam. The deflected fraction consists of particles which upon entering the crystal have transverse energies small enough that they can pass through the center of the crystal, where the depth of the effective potential is significantly smaller than in a straight crystal. These particles move in the region of lower electron density, and so they form a maximum of the channeled particles at low energy losses.

Increase of the bending angle of the crystal restricts the transverse energies of the deflected particles at the entrance to the crystal even more strongly. In Fig. 17c we compare the energy-loss spectra of the deflected fraction of particles for two different bending angles. Their behavior agrees well with experiment.[67] For large crystal bending angle the width of the spectrum is smaller, because in moving with smaller amplitudes in the channel the particles encounter a lower electron density, and so there is less spread in their energy losses.

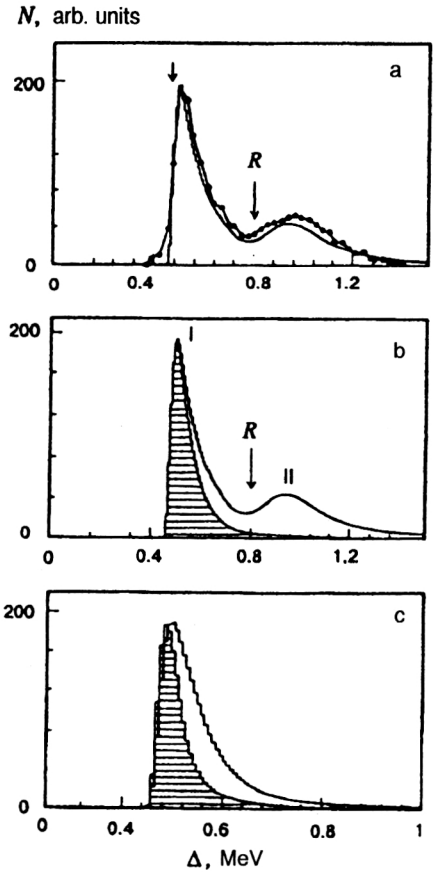

FIG. 17. (a) and (b) Calculated spectrum of ionization energy losses of 450-GeV protons at the entrance to a Si crystal oriented with (111) planes parallel to the beam axis. The arrow R indicates the most probable losses in the misoriented case. (a) Points from a CERN experiment; (b) shaded histogram showing the spectrum of the deflected fraction of the beam for bending angle 1.4 mrad; (c) spectra of the deflected fraction for various bending angles: 1.4 mrad and 8.9 mrad (shaded).

7. RADIATION OF CHANNELED PARTICLES

Synchrotron radiation, i.e., the radiation of relativistic charged particles undergoing periodic motion in a circular trajectory in a magnetic field, has been well studied and is used for scientific and applied purposes.[71] Synchrotron radiation has a quasicontinuous spectrum and occurs mainly in the frequency range $0-5\omega_c$, where ω_c is the characteristic radiation frequency,

$$\omega_c=3\Omega_0\gamma^3/2, \quad \Omega_0=v/R, \tag{79}$$

and Ω_0 is the angular frequency of the circular motion.

The radiation of relativistic particles moving along an arc of a circle, i.e., radiation in a short magnet, has been studied in Ref. 72. For arc length $L\leq l_c$, where $l_c=R\gamma^{-1}$ is

the coherence length for radiation at frequency ω_c in the motion of a particle along an arc of a circle of radius R, the spectrum has a maximum at $\omega=0$, like the radiation spectrum for the case of a short magnet. As the arc length increases the radiation spectrum is transformed into a synchrotron spectrum. The formation of the synchrotron spectrum with maximum at $\omega\simeq\omega_c$ is complete when the arc length exceeds l_c by more than an order of magnitude.

Radiation of high spectral density and directivity arises in the channeling of relativistic charged particles in a crystal.[73] The properties of the radiation depend on the relative sizes of the characteristic radiation angle $\theta_{\text{eff}}=\gamma^{-1}$ determining the width of the angular distribution of the radiation in the relativistic case and the deflection angles in the particle motion. The maximum deflection angle for channeled particles is determined by the critical channeling angle ϑ_c. For $\vartheta_c\gamma\ll 1$ the radiation from channeled particles is dipole radiation and is formed by the entire trajectory of the particle in the crystal. In the opposite case, when $\vartheta_c\gamma\gg 1$, the radiation is synchrotron radiation and is formed on a segment of the trajectory smaller than the particle oscillation length λ in the channel.[74]

The emission from particles undergoing planar channeling in a straight crystal has characteristics similar to the radiation in undulators, but in the former the frequency of the transverse particle oscillations is determined by the planar potential of the crystal and depends on the particle energy, $\omega_0=c\vartheta_c/l\sim\gamma^{-1/2}$ (Ref. 73). The emission from channeled particles in a given direction θ occurs at frequencies (radiation harmonics)

$$\omega_k(\theta)=\frac{k\omega_0}{1-\bar{\beta}\cos\theta}\simeq\frac{k\omega_u}{1+\gamma^2\theta^2+0.5\gamma^2\beta_m^2}, \qquad (80)$$

$$\omega_u=2\gamma^2\omega_0,$$

which grow with the particle energy as $\omega_u\sim\gamma^{3/2}$.

In planar channeling in a uniformly bent crystal, a particle undergoing oscillations in the channel field moves along an equilibrium orbit which is the arc of a circle. Therefore, changes arise in the radiation spectra of particles channeled in a bent crystal, owing to the appearance of the synchrotron radiation produced when the particles move on the arc of a circle along the bent planar channels. The general features of the effect of the crystal bending on the radiation of channeled particles were determined in Ref. 75. The bending of the crystal introduces fundamental changes in the radiation of channeled particles only in the case $\vartheta_c\gamma\leq 1$. The radiation of channeled particles in a bent crystal is quasiundulator radiation, where

$$l_c\gg\lambda. \qquad (81)$$

When the reverse inequality holds, the radiation is quasisynchrotron radiation.

The features of the spectral distribution of the radiation of channeled particles in a bent crystal arising from the interference of two emission mechanisms—undulator and synchrotron—have been studied in Refs. 76 and 77 by computer modeling.

7.1. The radiation intensity

The total intensity of the radiation in the planar channeling of particles in a crystal is determined by the acceleration that the particles acquire in the average electric field of the planar channel:

$$I(x)=\frac{2e^2}{3m^2c^3}\gamma^2|\nabla U(x)|^2. \qquad (82)$$

The intensity of the radiation of channeled particles in a bent crystal, averaged over trajectories and the particle ensemble, in the case where a parallel beam enters bent planar channels tangentially is the following when the parabolic approximation is used for the channel potential:[76]

$$I(R)=\frac{2e^2}{3m^2c^3}\gamma^2\left(\frac{2U_0}{l^2}\right)^2\left[\frac{l^2}{6}+\frac{x_0^2-2x_0l}{6}+x_0^2\right]$$

$$=I_{\text{st}}+I_a(R)+I_s(R), \qquad (83)$$

where I_{st} is the intensity of the channeled-particle radiation in a straight crystal, and I_a and I_s are terms describing the change in the radiation intensity when the crystal is bent due to the decrease of the maximum particle oscillation amplitude in the channel and the shift of x_0 of the equilibrium orbit toward the outer wall in the region of nonzero channel electric field strength. The last term determines the intensity of the particle synchrotron radiation for motion along the arc of a bent channel:

$$I_s(R)=\frac{2}{3}\frac{e^2c}{R^2}\beta^4\gamma^4, \qquad (84)$$

which grows with decreasing radius as R^{-2}. The bending of the crystal leads to decrease of particle capture into the channeling regime, and so the radiation yield from the channeled fraction of the beam is not increased.[76]

7.2. The radiation spectrum

The general expression for the spectral–angular distribution of energy radiated by a particle in the wave zone[78,79] can be written as

$$\frac{d^2W}{d\hbar\omega d\Omega}=\frac{\alpha}{4\pi^2}|\mathbf{n}\times\mathbf{l}_f|^2, \qquad (85)$$

$$\mathbf{l}_f=\mathbf{F}_k(t)\exp[iF_a(t)]\Big|_{t_1}^{t_2}-i\omega\int_{t_1}^{t_2}\boldsymbol{\beta}(t)\exp[iF_a(t)]dt,$$

$$\mathbf{F}_k(t)=\frac{\boldsymbol{\beta}(t)}{1-\mathbf{n}\boldsymbol{\beta}(t)},\quad F_a(t)=\omega[t-\mathbf{nr}(t)/c],$$

where $\alpha=e^2/\hbar c$, $\mathbf{n}$ is a unit vector in the direction of the emission, $\mathbf{r}$ is the particle radius vector, and t_1 and t_2 are the instants at which the particle enters and leaves the crystal. It is assumed that the particle moves with constant velocity outside the crystal. The equation for the trajectory of a channeled particle in a bent crystal in the parabolic approximation for the channel potential has the form

$$\mathbf{r}(t)=\{r_p(t)\cos\varphi_p(t), r_p(t)\sin\varphi_p(t), 0\}, \qquad (86)$$

$$r_p(t)=R+x_m\sin\omega_0 t,$$

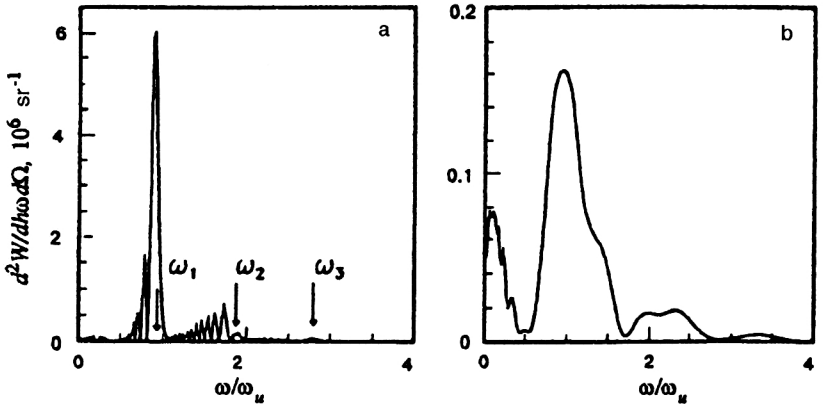

FIG. 18. Radiation spectra of a positron with $\gamma = 10^4$ in the orbital plane for channeling in the (110) channel of a bent silicon crystal with oscillation amplitude $x_m = 0.4l$: (a) $R = 76.4$ cm, $l_c \geqslant 11\lambda$, $\omega_u/\omega_c = 100$; (b) $R = 7.64$ cm, $l_c \geqslant \lambda$, $\omega_u/\omega_c = 10$.

$$\varphi_p(t) = \frac{S(t)}{R} = \frac{v}{R}\left[\frac{\bar{\beta}}{\beta}t - \frac{1}{8\omega_0}\left(\frac{\beta_m}{\beta}\right)^2 \sin 2\omega_0 t\right],$$

where $S(t)$ is the path traveled by the particle along the channel, and the other notation is the same as in (14). The integral in (85) was divided into N intervals of length much smaller than the oscillation period, on which the change of the particle velocity can be neglected, and was calculated analytically using a linear approximation for $F_a(s)$ on each interval.

In Fig. 18 we show the calculated radiation spectra of a positron with $\gamma = 10^4$ for channeling in the (110) channel of a bent silicon crystal with oscillation amplitude $x_m = 0.4l$ in a direction lying in the plane of the orbit. For small bending of the crystal (a), when $l_c \geqslant 10\lambda$ and $\omega_u/\omega_c = 100$, the maxima observed in the spectra are easily identified with the radiation harmonics in a straight crystal (indicated by the arrows). However, subharmonics at lower frequencies appear. For strong bending of the crystal (b), when $l_c \geqslant \lambda$ and $\omega_u/\omega_c = 10$, in addition to the principal maximum at the first radiation harmonic in a straight crystal, the spectrum contains an additional maximum at low frequencies due to the synchrotron radiation of particles moving along an arc of a bent channel.

The radial oscillations which a channeled particle undergoes in a bent crystal over the formation length l_c of the synchrotron radiation spectrum lead to the appearance of oscillations in the spectra. Here the oscillation period in the synchrotron radiation spectrum of a channeled particle decreases with decreasing bend radius of the crystal, owing to the decrease of the number of oscillations that the particle undergoes in the channel over the formation length of the radiation.

The radial oscillations of a channeled particle also cause the synchrotron radiation spectra to depend on the observation azimuth in the angular range $\Delta\varphi_\lambda = \lambda/R = \gamma^{-1}\lambda/l_c$, owing to the change of phase of the particle oscillations at the point where the orbit is tangent to the observation direction. In Fig. 19 we show the spectra for the two directions in the orbital plane for which the particle oscillation phases are separated by $\Delta\phi = \pi$, when the maximum positive and negative shifts of the particle from the orbit occur. The oscillations in the radiation spectra are the inverses of each other. For this reason they are mostly damped out upon averaging over the azimuth, when either the detector has azimuthal dimensions larger than $\Delta\varphi_\lambda$, or the particles in the channel have mixed oscillation phases. Such mixing does actually occur, owing to the anharmonicity of the planar-channel potential and multiple scattering. If a narrow beam with spread much smaller than the critical channeling angle is used along with a detector with window smaller than $\Delta\varphi_\lambda$, it is possible to understand the process of phase mixing in an ensemble of channeled particles on the basis of the quasisynchrotron radiation spectra of channeled positrons.

In Fig. 20 we show the radiation spectra, integrated over angle, of a positron with $\gamma = 10^4$ for channeling with amplitude $x_m = 0.4l$ in a bent crystal. For small bending (a) the spectrum is close to that in a straight crystal with maxima determined by the emission at the first and second harmonics. Bending leads only to oscillations in the spectrum. In the case of strong bending (b) the resulting synchrotron radiation forms a maximum roughly equal to the radiation maximum at the first harmonic.

Radiation in a bent crystal was later studied using the semiclassical operator formalism.[80] Again, oscillations were found in the radiation spectra due to the two radiation mechanisms. For $R \to \infty$ the expressions obtained in Ref. 80

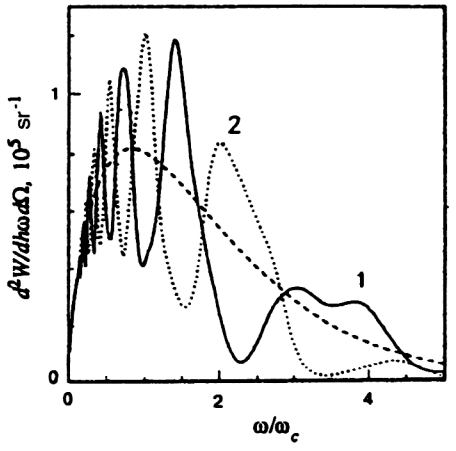

FIG. 19. Synchrotron part of the radiation spectrum of a positron with $\gamma = 10^4$ in channeling with $x_m = 0.4l$ in the (110) channel of a bent silicon crystal for two azimuthal directions in the orbital plane, $R = 7.64$ cm. The dashed line is the spectrum of ordinary synchrotron radiation.

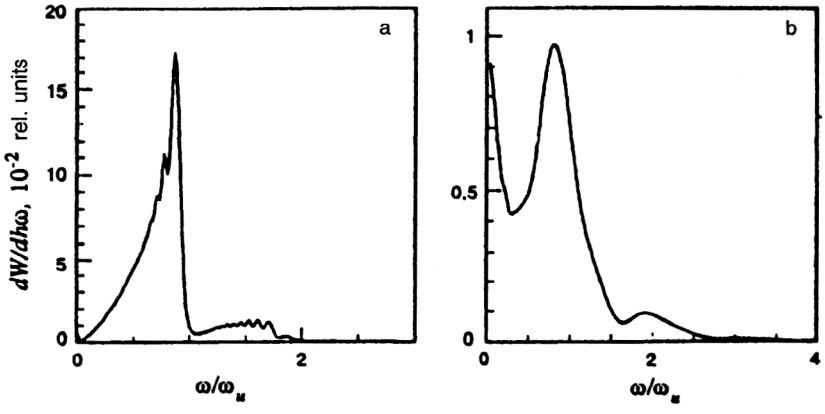

FIG. 20. Integrated radiation spectrum of a positron with $\gamma = 10^4$ for channeling in the (110) channel of a bent silicon crystal with $x_m = 0.4l$: (a) $R = 76.4$ cm, $l_c \geqslant 11\lambda$; (b) $R = 7.64$ cm, $l_c \geqslant \lambda$.

become the well known expressions for radiation in a straight crystal.

The frequency and intensity of synchrotron radiation depend strongly on the relativistic factor of the particles, which can be used to identify them. The possibility of particle identification by recording the synchrotron radiation arising in the channeling of particles in a bent crystal was discussed in Ref. 16.

8. THE SPIN PRECESSION OF CHANNELED PARTICLES

In an electric field $\mathscr{E}$ the spin vector of a particle precesses about the pseudovector $\boldsymbol{\nu} = \mathscr{E} \times \mathbf{v}$ normal to the plane of the motion.[81] In planar channeling in a crystal a particle moves in a strong transverse electric field, which, however, is strongly nonuniform and changes direction on opposite sides of the channel (planes). The trajectory of a positively charged particle oscillates between the planes, and the rotation direction of its momentum and magnetic moment varies periodically. There is no deflection of the particle momentum and spin when the ensemble of channeled particles is averaged over. This also follows from the fact that the average field strength along the particle trajectory is equal to zero in this case.

The average strength of the electric field acting on a channeled particle in a bent crystal is nonzero, owing to the displacement of the equilibrium orbit from the center of the channel. This field, which is perpendicular to the particle momentum, also induces deflection of the particle by the crystal bending angle. As was first shown in Ref. 82, the electric field of the planar channels of a bent crystal, which is preferentially directed in the particle channeling region, leads to significant spin rotation of the channeled particles.

The Bargman–Michel–Telegdi equation, which describes the behavior of the spin of a relativistic particle in an electromagnetic field, was used in Ref. 83 to establish the existence of a simple relation between the precession angular velocity of the spin Ω and the momentum Ω_0 of a particle moving in an electric field:

$$\Omega = \left[\frac{g-2}{2}\frac{\gamma^2-1}{\gamma} + \frac{\gamma-1}{\gamma}\right]\Omega_0, \tag{87}$$

where g is the Landé factor. When the particle energy hardly changes during motion in the field, the same relation also holds between the rotation angles of the particle spin ϑ and momentum ϑ_0, i.e., for $\gamma \gg 1$ we have

$$\vartheta = \vartheta_0 \gamma (g-2)/2. \tag{88}$$

Equation (88) determines the spin precession angle of a particle passing through a bent crystal in the planar-channeling regime in terms of the bending angle of the crystal.

The angular spread of the spin precession of channeled particles deflected by a crystal is due to the difference between the real crystal potential and the averaged potential, and also to scattering on the crystal electrons. The precession angle of particles which have passed through a crystal is significantly affected by the possibility that they travel along part of the path without being in the channeling regime: the particles can be captured into the channeling regime or dechanneled in the crystal volume. Kinetic equations describing the evolution of the particle distribution in the spin orientation during passage through a bent crystal were obtained in Ref. 84, taking into account multiple scattering. They can be used to estimate the spectrum of particle spin rotation angles.

The measurement of the particle spin precession angle in deflection by a bent crystal can be used to determine the magnetic moments of short-lived particles.[85] The method has already been successfully tested in an experiment at Fermilab to measure the spin precession angle of Σ^+ hyperons.[86]

The strength of the electric field acting on a channeled particle in a crystal in the particle rest frame, $\mathscr{E}' = \gamma\mathscr{E}$, can reach the critical value $\mathscr{E}_0 = m^2c^3/e\hbar = 1.32 \times 10^{16}$ V/cm at high particle energies. Quantum electrodynamics predicts that the particle anomalous magnetic moment μ' changes in such fields. The change of μ' can be detected by measuring the precession angle in the passage through a bent crystal of channeled positrons with energy above 100 GeV, attainable in secondary beams of proton accelerators.[87]

9. POLARIZATION PHENOMENA

Quantum effects in the synchrotron radiation of high-energy electrons and positrons can be used to obtain polarized $e^{\pm}$ beams of energy ~ 10 GeV in electron storage rings.[71] Radiative transitions between states with different

particle spin projections on the direction of the magnetic field cause the particles to accumulate in the level of lowest energy, i.e., the positron spins are oriented along the field and the electron spins opposite to the field. In addition, the quantum nature of synchrotron radiation is manifested in the strong dependence of the intensity of radiation without change of polarization on the orientation of the particle spin relative to the field, which can also be used to separate particles according to their spins.[88]

In an electric field $\mathscr{E}$ the dependence of the probability for radiation with spin flip on the initial orientation of the spin relative to the pseudovector $\boldsymbol{\nu}$ can also lead to the appearance of a transverse polarization of the electrons and positrons. In planar channeling in a straight crystal, the direction of the predominant spin orientation for the channeled particles varies periodically, and the average polarization of the emitting particles will be zero. In a bent crystal, owing to the shift of the equilibrium orbit toward the outer wall of the channel, the channeled particles spend most of their time in regions with a single direction of the average planar field, which can lead to radiative polarization of channeled $e^{\pm}$ (Ref. 87).

The appearance of quantum effects in the radiation for particle motion in an electric field is determined by the parameter $\chi=\gamma\mathscr{E}/\mathscr{E}_0$, equal to the ratio of the electric field strength in the particle rest frame to the critical field strength. The probability for radiation with spin flip increases with increasing χ. In storage rings $\chi\ll 1$. Radiative processes with spin flip are relatively rare, and polarization occurs over the course of many rotations, which is possible owing to the cancellation of the general radiation energy losses, which significantly exceed the losses to radiation with particle spin flip.

In channeling in a bent crystal cancellation of the losses is impossible, and a significant polarization can be obtained only for high-energy $e^{\pm}$, when $\chi\geqslant 1$. Since here the energy of the emitted photons is comparable to the $e^{\pm}$ energy, the polarization is obtained at the cost of a significant decrease of the particle energy, and so the crystal should be as short as possible. The problem of $e^{\pm}$ polarization in channeling in a bent crystal taking into account multiple scattering and radiation energy losses of the particles has been studied in Ref. 89, using the kinetic approach. The calculations show that the degree of polarization can reach 15–30% for $e^{\pm}$ beams in the TeV range.

A bent crystal can be used not only for the radiative polarization of $e^{\pm}$, but also for photon conversion into polarized $e^{+}e^{-}$ pairs. When a photon creates an electron–positron pair in a uniform electric field, the particles can acquire a high degree of polarization, with the positron spin parallel to the pseudovector $\boldsymbol{\nu}$ and the electron spin antiparallel to it.[18] Since bending of the crystal causes an electric field of a single direction to dominate in the channel cross section in the $e^{\pm}$ channeling region, and since pair production in a uniform field is a local process whose contribution is important for $\kappa=\hbar\omega\mathscr{E}/(mc^2\mathscr{E}_0)\geqslant 1$, where ω is the photon frequency, the particles of pairs created by photons in a bent crystal and captured into the channeling regime will possess a high degree of polarization.[18] In Ref. 18 it was suggested that this process also be used in the secondary photon beams of proton accelerators, for example, the Tevatron. It is estimated that it will be possible to obtain 10^{-3}–10^{-2} transversely polarized $e^{\pm}$ of energy $\sim$100 GeV per photon.

10. CONCLUSION

The idea of deflecting channeled particles by a bent crystal, which at first seemed quite exotic, has proved to be experimentally feasible and quite fruitful. In addition to the particle channeling effect itself, the phenomenon of volume capture of particles into the channeling regime in a bent crystal has been discovered experimentally and studied. This in turn has stimulated the detailed study of the volume capture of particles in a straight crystal, which has shed light on the role of volume capture and recapture processes in increasing the observed particle dechanneling length. The deflection of quasichanneled particles by a bent crystal in the direction opposite to the bend (volume reflection) was discovered by modeling.

In the planar channeling of relativistic positrons in a bent crystal, the situation is realized in which two radiation mechanisms operate: the quasiundulator mechanism due to particle oscillations in the channel, and the synchrotron mechanism due to the curvature of the channel itself. The interference of these two mechanisms leads to the appearance of oscillations in the radiation spectra.

When a crystal is bent the electric field of the planar channels acquires a preferential direction in the channeling region owing to the displacement of the equilibrium orbit from the center of the channel. This leads to significant spin rotation angles of the channeled particles and the possibility of radiative polarization of high-energy channeled electrons and positrons.

Of the many possible applications of bent crystals for steering beams of charged particles, the most important is their use in loss-localization systems for colliders, which effect the extraction of particles of the beam halo for simultaneous fixed-target experiments and also significantly reduce the radiation background of collider experiments.

Applications of bent crystals in high-energy physics appear very promising. One is the measurement of the magnetic moments of short-lived particles on the basis of the spin precession angle in a bent crystal.

In conclusion, I would like to deeply thank É. N. Tsyganov and S. A. Vorob'ev (deceased), with whom many of the results discussed in this review were obtained. I also thank A. M. Baldin, V. V. Glagolev, and A. D. Kovalenko for their support and interest in this study.

[1)]The shadow effect is also observed in oriented crystals; see A. F. Tulinov, Usp. Fiz. Nauk **87**, 585 (1965) [Sov. Phys. Usp. **8**, 864 (1966)].

[1] J. Lindhard, K. Dan. Vidensk. Selsk. Mat. Fys. Medd. **34**, No. 1 (1965).
[2] E. N. Tsyganov, Preprints TM-682, TM-684, Fermilab, Batavia (1976).
[3] A. M. Taratin, E. N. Tsyganov, and S. A. Vorob'ev, Pis'ma Zh. Tekh. Fiz. **4**, 947 (1978) [Sov. Tech. Phys. Lett. **4**, 381 (1978)]; A. M. Taratin, E. N. Tsyganov, and S. A. Vorobiev, Phys. Lett. A **72**, 145 (1979).

[4]A. S. Vodop'yanov, V. M. Golovatyuk *et al.*, Pis'ma Zh. Éksp. Teor. Fiz. **30**, 474 (1979) [JETP Lett. **30**, 442 (1979)].
[5]Yu. N. Adishchev *et al.*, Pis'ma Zh. Éksp. Teor. Fiz. **30**, 430 (1979) [JETP Lett. **30**, 402 (1979)].
[6]J. Bak *et al.*, Phys. Lett. B **93**, 505 (1980).
[7]V. V. Avdeĭchikov *et al.*, Brief Commun. No. 1-84, JINR, Dubna (1984), p. 3 [in Russian].
[8]A. A. Aseev, M. D. Bavizhev *et al.*, Preprint 89-57, IHEP, Serpukhov (1989) [in Russian].
[9]V. M. Biryukov, V. I. Kotov, and Yu. A. Chesnokov, Usp. Fiz. Nauk **164**, 1017 (1994) [Phys. Usp. **37**, 937 (1994)].
[10]J. F. Bak *et al.*, Nucl. Phys. B **242**, 1 (1984); A. Baurichter *et al.*, Nucl. Instrum. Methods Phys. Res. B **119**, 172 (1996).
[11]H. Akbari *et al.*, Phys. Lett. B **313**, 491 (1993); K. Elsener *et al.*, Nucl. Instrum. Methods Phys. Res. B **119**, 215 (1996).
[12]W. M. Gibson *et al.*, Nucl. Instrum. Methods Phys. Res. B **2**, 54 (1984).
[13]C. T. Murphy, R. Carrigan *et al.*, Nucl. Instrum. Methods Phys. Res. B **119**, 231 (1996).
[14]L. I. Bel'zer, V. A. Bodyagin *et al.*, Preprint R1-87-654, JINR, Dubna (1987) [in Russian]; in *Proceedings of the All-Union Conf. on Problems in the Use of Particle Channeling by Crystals in High-Energy Physics* [in Russian], Protvino, 1991, p. 45.
[15]E. Tsyganov, A. Taratin, and A. Zinchenko, Fiz. Élem. Chastits At. Yadra **27**, 675 (1996) [Phys. Part. Nuclei **27**, 279 (1996)].
[16]M. Bavizhev and V. Biryukov, Preprint SSCL-N-774 (1991).
[17]R. A. Carrigan, Jr., W. M. Gibson, C. R. Sun, and E. N. Tsyganov, Nucl. Instrum. Methods Phys. Res. **194**, 205 (1982).
[18]V. G. Baryshevskiĭ and V. V. Tikhomirov, Usp. Fiz. Nauk **159**, 455 (1989) [Sov. Phys. Usp. **32**, 972 (1989)].
[19]R. A. Carrigan, Jr. and W. M. Gibson, in *Coherent Radiation Sources*, Topics in Current Physics, Vol. 38, edited by A. W. Saenz and H. Uberall (Springer-Verlag, Berlin, 1985), p. 61.
[20]R. A. Carrigan, Jr., in *Relativistic Channeling*, edited by R. A. Carrigan, Jr. and J. Ellison (Plenum Press, New York, 1987), p. 339.
[21]V. M. Biryukov, Yu. A. Chesnokov, and V. I. Kotov, *Crystal Channeling and Its Application at High-Energy Accelerators* (Springer-Verlag, Berlin, 1997).
[22]N. P. Kalashnikov, *Coherent Interactions of Charged Particles in Single Crystals* [in Russian] (Atomizdat, Moscow, 1981).
[23]Yu. L. Pivovarov and S. A. Vorob'ev, Dokl. Akad. Nauk SSSR **256**, 837 (1981) [Sov. Phys. Dokl. **26**, 186 (1981)].
[24]J. S. Forster *et al.*, Nucl. Phys. B **318**, 301 (1989).
[25]A. M. Taratin, Report R1-96-262, JINR, Dubna (1996) [in Russian].
[26]A. P. Pathak, Phys. Rev. B **13**, 4688 (1976).
[27]V. V. Kaplin and S. A. Vorob'ev, Pis'ma Zh. Tekh. Fiz. **4**, 196 (1978) [Sov. Tech. Phys. Lett. **4**, 78 (1978)].
[28]A. M. Taratin, Yu. M. Filimonov, E. G. Vyatkin, and S. A. Vorobiev, Phys. Status Solidi B **100**, 273 (1980).
[29]A. M. Taratin and S. A. Vorobiev, Phys. Status Solidi B **107**, 521 (1981).
[30]M. D. Bavizhev, V. M. Biryukov, and Yu. G. Gavrilov, Zh. Tekh. Fiz. **61**, No. 2, 136 (1991) [Sov. Phys. Tech. Phys. **36**, 203 (1991)].
[31]A. M. Taratin and S. A. Vorobiev, Phys. Lett. A **119**, 425 (1987); Nucl. Instrum. Methods Phys. Res. B **26**, 512 (1987).
[32]V. V. Beloshitskiĭ and M. A. Kumakhov, Dokl. Akad. Nauk SSSR **212**, 846 (1973) [Sov. Phys. Dokl. **18**, 652 (1973)].
[33]A. M. Taratin and S. A. Vorobiev, Nucl. Instrum. Methods Phys. Res. B **47**, 247 (1990).
[34]T. Waho, Phys. Rev. B **14**, 4830 (1976).
[35]A. G. Bonch-Osmolovskiĭ and M. I. Podgoretskiĭ, Report R2-11634, JINR, Dubna (1978) [in Russian].
[36]J. S. Forster, in *Relativistic Channeling*, edited by R. A. Carrigan, Jr. and J. Ellison (Plenum Press, New York, 1987), p. 39.
[37]H. Kudo, Nucl. Instrum. Methods Phys. Res. **189**, 609 (1981).
[38]J. A. Ellison and S. T. Picraux, Phys. Lett. A **83**, 271 (1981).
[39]J. A. Ellison, Nucl. Phys. B **206**, 205 (1982).
[40]J. A. Ellison *et al.*, Nucl. Instrum. Methods Phys. Res. B **2**, 9 (1984).
[41]W. M. Gibson, in *Relativistic Channeling*, edited by R. A. Carrigan, Jr. and J. Ellison (Plenum Press, New York, 1987), p. 101.
[42]A. D. Kovalenko, V. A. Mikhailov, A. M. Taratin *et al.*, JINR Rapid Commun. No. 4[72], JINR, Dubna (1995), p. 9.
[43]A. M. Taratin, S. A. Vorobiev, M. D. Bavizhev, and I. A. Yazynin, Nucl. Instrum. Methods Phys. Res. B **58**, 103 (1991).
[44]V. M. Biryukov, Nucl. Instrum. Methods Phys. Res. B **53**, 202 (1991).
[45]G. Arduini *et al.*, Phys. Rev. Lett. **79**, 4182 (1997).
[46]N. A. Kudryashov, S. V. Petrovskiĭ, and M. N. Strikhanov, Yad. Fiz. **48**, 666 (1988) [Sov. J. Nucl. Phys. **48**, 426 (1988)].
[47]A. M. Taratin, Preprint E1-97-320, JINR, Dubna (1997).
[48]A. M. Kol'chuzhkin and V. V. Uchaĭkin, *Introduction to the Theory of the Passage of Particles Through Matter* [in Russian] (Atomizdat, Moscow, 1978).
[49]H. A. Bethe, Phys. Rev. **89**, 1256 (1953).
[50]Particle Data Group, Phys. Rev. D **50**, 1173 (1994).
[51]A. M. Taratin and S. A. Vorob'ev, Zh. Tekh. Fiz. **55**, 1598 (1985) [Sov. Phys. Tech. Phys. **30**, 927 (1985)]; A. M. Taratin and S. A. Vorobiev, Phys. Status Solidi B **133**, 511 (1986); Phys. Lett. A **115**, 398 (1986).
[52]M. Kitagawa and Y. H. Ohtsuki, Phys. Rev. B **8**, 3117 (1973).
[53]V. A. Ryabov, *The Channeling Effect* [in Russian] (Énergoatomizdat, Moscow, 1994).
[54]V. Biryukov, Phys. Rev. E **51**, 3522 (1995).
[55]V. A. Andreev *et al.*, Pis'ma Zh. Éksp. Teor. Fiz. **36**, 340 (1982) [JETP Lett. **36**, 415 (1982)]; V. M. Samsonov, in *Relativistic Channeling*, edited by R. A. Carrigan, Jr. and J. Ellison (Plenum Press, New York, 1987), p. 129.
[56]N. K. Bulgakov *et al.*, Report 1-83-725, JINR, Dubna (1983) [in Russian].
[57]V. V. Beloshitskiĭ and V. A. Starostin, Pis'ma Zh. Tekh. Fiz. **14**, 722 (1988) [Sov. Tech. Phys. Lett. **14**, 321 (1988)].
[58]A. M. Taratin, Nucl. Instrum. Methods Phys. Res. B **95**, 243 (1995).
[59]E. A. Mazur and M. N. Strikhanov, in *Proceedings of the Thirteenth All-Union Meeting on the Physics of the Interaction of Charged Particles With Crystals* [in Russian] (Moscow State University Press, Moscow, 1984), p. 8.
[60]M. A. Kumakhov, Preprint L-122178, Institute of Nuclear Physics, Moscow State University, Moscow (1970) [in Russian].
[61]Yu. A. Chesnokov *et al.*, Nucl. Instrum. Methods Phys. Res. B **69**, 247 (1992).
[62]V. M. Biryukov *et al.*, Nucl. Instrum. Methods Phys. Res. B **73**, 153 (1993).
[63]O. I. Sumbaev, Preprint No. 1201, Leningrad Nuclear Physics Institute, Leningrad (1986) [in Russian].
[64]M. Mannami *et al.*, Nucl. Instrum. Methods Phys. Res. B **33**, 62 (1988).
[65]V. M. Biryukov *et al.*, Nucl. Instrum. Methods Phys. Res. B **73**, 153 (1993); V. M. Biryukov, Phys. Lett. A **205**, 343 (1995).
[66]H. Esbensen *et al.*, Phys. Rev. B **18**, 1039 (1978).
[67]S. P. Møller *et al.*, Nucl. Instrum. Methods Phys. Res. B **84**, 434 (1994).
[68]N. A. Kudryashov *et al.*, Nucl. Phys. B **324**, 277 (1989); Phys. Status Solidi B **157**, 531 (1990).
[69]A. M. Taratin, Nucl. Instrum. Methods Phys. Res. B **119**, 156 (1996).
[70]H. Esbensen and J. Golovchenko, Nucl. Phys. A **298**, 382 (1978).
[71]I. M. Ternov and V. V. Mikhaĭlin, *Synchrotron Radiation. Theory and Experiment* [in Russian] (Énergoatomizdat, Moscow, 1986).
[72]V. G. Bagrov, I. M. Ternov, and N. I. Fedosov, Zh. Éksp. Teor. Fiz. **82**, 1442 (1982) [Sov. Phys. JETP **55**, 835 (1982)].
[73]M. A. Kumakhov, *Radiation of Channeled Particles in Crystals* [in Russian] (Énergoatomizdat, Moscow, 1986).
[74]V. N. Baĭer, V. M. Katkov, and V. M. Strakhovenko, *Electromagnetic Processes at High Energies in Oriented Single Crystals* [in Russian] (Nauka, Novosibirsk, 1989).
[75]Yu. A. Bashmakov, Radiat. Eff. **56**, 55 (1981).
[76]A. M. Taratin, Zh. Tekh. Fiz. **59**, 138 (1989) [Sov. Phys. Tech. Phys. **34**, (1989)]; A. M. Taratin and S. A. Vorobiev, Nucl. Instrum. Methods Phys. Res. B **31**, 551 (1988).
[77]A. M. Taratin and S. A. Vorobiev, Nucl. Instrum. Methods Phys. Res. B **42**, 41 (1989).
[78]L. D. Landau and E. M. Lifshitz, *The Classical Theory of Fields*, 4th English ed. (Pergamon Press, Oxford, 1975) [Russ. original, 6th ed., Nauka, Moscow, 1973].
[79]J. D. Jackson, *Classical Electrodynamics*, 2nd ed. (Wiley, New York, 1975) [Russ. transl. of 1st ed., IL, Moscow, 1965].
[80]V. A. Arutyunov, N. A. Kudryashov, M. N. Strikhanov, and V. M. Samsonov, Zh. Tekh. Fiz. **61**, No. 32 (1991) [Sov. Phys. Tech. Phys. **36**, (1991)]; V. A. Arutyunov *et al.*, Nucl. Phys. B **363**, 283 (1991).
[81]V. G. Berestetskiĭ, E. M. Lifshitz, and L. P. Pitaevskiĭ, *Quantum Electrodynamics*, 2nd ed. (Pergamon Press, Oxford, 1982) [Russ. original, Nauka, Moscow, 1980].
[82]V. G. Baryshevskiĭ, Pis'ma Zh. Tekh. Fiz. **5**, 182 (1979) [Sov. Tech. Phys. Lett. **5**, 73 (1979)].
[83]V. L. Lyuboshits, Yad. Fiz. **31**, 986 (1980) [Sov. J. Nucl. Phys. **31**, 509 (1980)].

[84] N. A. Kudryashov *et al.*, Yad. Fiz. **51**, 173 (1990) [Sov. J. Nucl. Phys. **51**, 110 (1990)].
[85] V. G. Baryshevskiĭ, in *Proceedings of the Fourteenth Winter School of the LIYaF* [in Russian] (Leningrad Nuclear Physics Institute, Leningrad, 1979), p. 158.
[86] V. V. Baublis *et al.*, Nucl. Instrum. Methods Phys. Res. B **90**, 112 (1994).
[87] V. G. Baryshevskiĭ and A. O. Grubich, Pis'ma Zh. Tekh. Fiz. **5**, 1527 (1979) [Sov. Tech. Phys. Lett. **5**, 648 (1979)].
[88] V. M. Baier, V. M. Katkov, and V. M. Strakhovenko, Phys. Lett. B **70**, 83 (1977).
[89] V. A. Arutyunov *et al.*, Nucl. Instrum. Methods Phys. Res. B **52**, 13 (1990).

Translated by Patricia A. Millard